
This is an electronic reprint of the original article.
This reprint may differ from the original in pagination and typographic detail.

Chen, Aifang; Liu, Junguo; Kummu, Matti; Varis, Olli; Tang, Qihong; Mao, Ganquan; Wang, Jie; Chen, Deliang

Multidecadal variability of the Tonle Sap Lake flood pulse regime

Published in:
Hydrological Processes

DOI:
[10.1002/hyp.14327](https://doi.org/10.1002/hyp.14327)

Published: 01/09/2021

Document Version
Peer-reviewed accepted author manuscript, also known as Final accepted manuscript or Post-print

Please cite the original version:
Chen, A., Liu, J., Kummu, M., Varis, O., Tang, Q., Mao, G., Wang, J., & Chen, D. (2021). Multidecadal variability of the Tonle Sap Lake flood pulse regime. *Hydrological Processes*, 35(9), Article 14327.
<https://doi.org/10.1002/hyp.14327>

This material is protected by copyright and other intellectual property rights, and duplication or sale of all or part of any of the repository collections is not permitted, except that material may be duplicated by you for your research use or educational purposes in electronic or print form. You must obtain permission for any other use. Electronic or print copies may not be offered, whether for sale or otherwise to anyone who is not an authorised user.

Multidecadal variability of the Tonle Sap Lake flood pulse regime

Running head: Flood pulse in the Tonle Sap Lake

Aifang Chen^{1,2}, Junguo Liu^{1*}, Matti Kummu³, Olli Varis³, Qihong Tang^{4,5}, Ganquan Mao¹, Jie Wang⁴, and Deliang Chen^{2*}

¹School of Environmental Science and Engineering, Southern University of Science and Technology, Shenzhen 518055, China

²Regional Climate Group, Department of Earth Sciences, University of Gothenburg, Gothenburg 40530, Sweden

³Water and Development Research Group, Aalto University, P.O. Box 15200, Aalto, Finland

⁴Key Laboratory of Water Cycle and Related Land Surface Processes, Institute of Geographic Sciences and Natural Resources Research, Chinese Academy of Sciences, Beijing 100101, China

⁵University of Chinese Academy of Sciences, Beijing 100101, China

*** Corresponding Author:** Junguo Liu (junguo.liu@gmail.com), Deliang Chen (deliang@gvc.gu.se)

Present address: School of Environmental Science and Engineering, Southern University of Science and Technology, Shenzhen 518055, China

Abstract

Tonle Sap Lake (TSL) is one of the world's most productive lacustrine ecosystems, driven by the Mekong River's seasonal flood pulse. This flood pulse and its long-term dynamics under the Mekong River basin's fast socio-economic development and climate change need to be identified and understood. However, existing studies fall short of sufficient time coverage or concentrate only on changes in water level (WL) that is only one of the critical flood pulse parameters influencing the flood pulse ecosystem productivity. Considering the rapidly changing hydroclimatic conditions in the Mekong basin, it is crucial to systematically analyze the changes in multiple key flood pulse parameters. Here, we aim to do that by using observed WL data for 1960 – 2019 accompanied with several parameters derived from a Digital Bathymetry Model. Results show significant declines of WL and inundation area from the late 1990s in the dry season and for the whole year, on top of increased subdecadal variability. Decreasing

(increasing) probabilities of high (low) inundation area for 2000 – 2019 have been found, in comparison to the return period of inundation area for 1986 – 2000 (1960 – 1986). The mean seasonal cycle of daily WL in dry (wet) season for 2000 – 2019, compared to that for 1986 – 2000, has shifted by 10 (5) days. Significant correlations and coherence changes between the WL and large-scale circulations (i.e., El Niño-Southern Oscillation [ENSO], Pacific Decadal Oscillation [PDO], and Indian Ocean Dipole [IOD]), indicate that the atmospheric circulations could have influenced the flood pulse in different time scales. Also, the changes in discharge at the Mekong mainstream suggest that anthropogenic drivers, such as hydropower operations, may have impacted the high water levels in the lake. Overall, our results indicate a declining flood pulse since the late 1990s.

Keywords: Water level, Inundation area, Climate change, Cambodia, Mekong

1. INTRODUCTION

Lakes provide freshwater resources and myriad ecosystem services. As a consequence of anthropogenic activities and climate change, however, lakes are frequently impacted, affecting the livelihood of local residents and communities (Junk, Bayley, & Sparks, 1989; Lamberts, 2006; Tang, 2020). Cambodia's Tonle Sap Lake (TSL), the largest lake in Southeast Asia, is one of the world's most productive lake-wetland systems (Arias, Holtgrieve, Ngor, Dang, & Piman, 2019; Campbell, Poole, Giesen, & Valbo-Jorgensen, 2006; MRC, 2010a; Poulsen, Ouch, Sintavong, Ubolratana, & Nguyen, 2002; Ziv, Baran, Nam, Rodriguez-Iturbe, & Levin, 2012), supporting about 1.7 million people (Keskinen, 2006; Salmivaara, Kummu, Varis, & Keskinen, 2016). The TSL has a unique 'flood pulse' (Arias, Cochrane, Norton, Killeen, & Khon, 2013; Junk et al., 1989), characterized by a seasonal rhythm of water level fluctuation between wet and dry seasons and resulting in a seasonally inundated floodplain (Arias et al., 2012; Frappart et al., 2006; MRC, 2010a).

This periodic and extensive floodplain provides unique habitats for many seasonally migratory fish species with replenishment of nutrients from the Mekong River (Arias et al., 2019; Campbell

et al., 2006; MRC, 2010a; Poulsen et al., 2002; Ziv et al., 2012). The TSL also offers provisions of freshwater resources (Chadwick, Juntopas, & Sithirith, 2008; Kummu, Sarkkula, Koponen, & Nikula, 2006) and maintains crucial habitats for many endangered species (Campbell et al., 2006; Uk et al., 2018). In addition, the lake's flood regime influences land cover change by, for instance, delineating the area of cropland in the floodplain and affecting the forest cover change (Arias et al., 2012; Halls et al., 2013; Salmivaara et al., 2016). Henceforth, TSL is the "heart of the lower Mekong", as the regional socio-economic development and ecosystem sustainability ultimately depend on the "flood pulse" (Junk et al., 1989; Keskinen, 2006; Lamberts, 2006; Salmivaara et al., 2016; Uk et al., 2018) (Figure 1).

Climate change and socio-economic development in the Mekong River Basin (MRB) have posed a soaring pressure on water resources in the past decades (Grumbine & Xu, 2011; Pokhrel et al., 2018; Uk et al., 2018; Wang, Feng, Liu, Hou, & Chen, 2020), through rapid development of hydropower dams with large reservoirs (Grumbine & Xu, 2011; Hecht, Lacombe, Arias, Dang, & Piman, 2019; Yun et al., 2020), irrigation (Floch & Molle, 2009; Kummu, 2009; Pokhrel et al., 2018), deforestation (Davis, Yu, Rulli, Pichdara, & D'Odorico, 2015; Hansen et al., 2013; Zeng et al., 2018), urbanization and cropland extension (Arias et al., 2019; Senevirathne, Mony, Samarakoon, & Kumar Hazarika, 2010; Song, Lim, Meas, & Mao, 2011). Strongly dominated by the Mekong mainstream flow, the flood pulse of the TSL would be influenced by any plausible changes to the mainstream flow (Kummu & Sarkkula, 2008; Kummu et al., 2014), resulting in destructions of the contiguous floodplain, inhibition of fish production, and thus the livelihood for the floodplain inhabitants (Keskinen, 2006; Lin & Qi, 2017; MRC, 2010b). Therefore, an adequate understanding of changes in the flood pulse is crucial for local and regional water management and sustainable development.

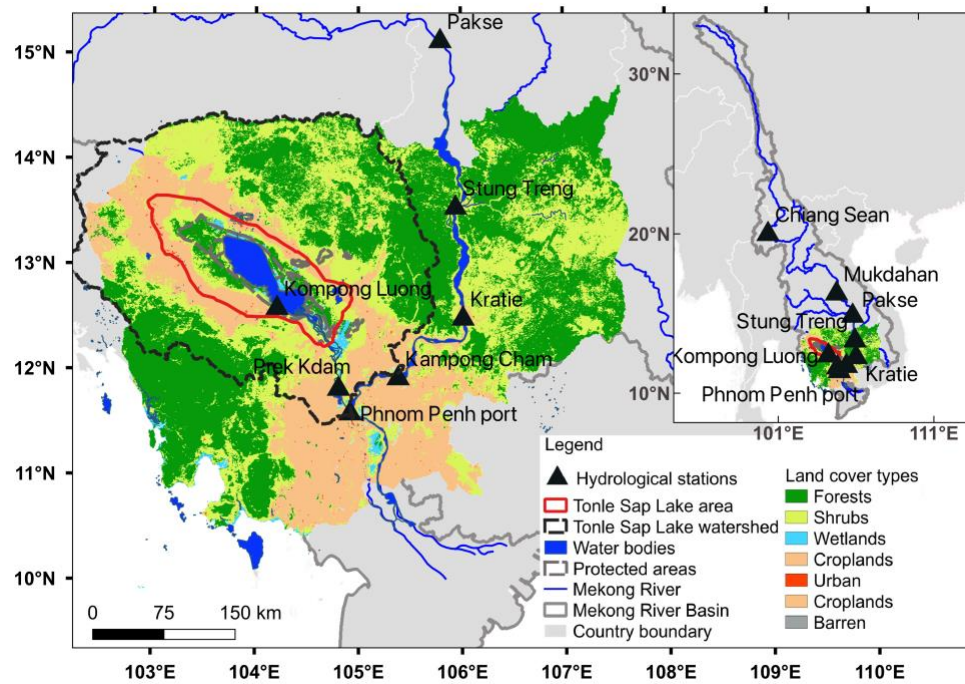


Figure 1. General information of the Tonle Sap Lake and Mekong River Basin. Data source: Land cover types in 2001 are from the MODerate resolution Imaging Sensor (MODIS) MCD12Q1; Hydrological stations are from Mekong River Commission (<http://www.mrcmekong.org/>); Other information is from the Open Development Cambodia (<https://opendevelopmentcambodia.net/>).

Many studies have investigated flood regime changes in the TSL, including water level (Frappart et al., 2006), water volume (Frappart et al., 2018; Kummu & Sarkkula, 2008; Siev, Paringit, Yoshimura, & Hul, 2016), flood extent (Arias et al., 2012; Dang, Cochrane, Arias, Van, & de Vries, 2016; Ji, Li, Luo, & He, 2018), and turbidity (Wang et al., 2020), by various means: remote sensing (e.g., MODIS, GRACE, RADARSAT, Landsat, ALOS/PALSAR (Dang et al., 2016; Ji et al., 2018; Sakamoto et al., 2007; Tangdamrongsub, Ditmar, Steele-Dunne, Gunter, & Sutanudjaja, 2016; Wang et al., 2020), Digital Bathymetry Model, and ground observed water level data (Arias et al., 2013; Kummu & Sarkkula, 2008). In general, for the flood regime of the TSL, these studies agree on an overall decreasing trend from 2000 in terms of water level (in the wet and dry seasons) (Ji et al., 2018; Lin & Qi, 2017) and inundation area (in the wet season) (Lin & Qi, 2017; Vichet et al., 2019).

High-resolution remote sensing data have played an important role in studying the flood pulse. These studies, targeted on the recent three decades at the earliest, have fallen short of sufficient time coverage to analyze the long-term changes as well as consistency of data sources. Recent articles have examined the water level change over a longer time period (Cochrane, Arias, & Piman, 2014; Guan & Zheng, 2021), but this is only one of the key parameters impacting flood pulse ecosystem productivity (Junk et al., 1989). Given the importance of the lake's flood pulse and potential changes to the lake caused by the climate and anthropogenic drivers in the MRB, more information is needed on the long-term changes of flood pulse's key parameters (Arias et al., 2019). We provide here a systematic analysis of all key flood pulse parameters and their changes over the past 60 years, i.e., 1960 – 2019, and thus reveal the much-needed information on changes in the flood pulse system. This is essential in understanding the potential impacts of the flood regime changes on Tonle Sap's ecosystem.

2. MATERIALS AND METHODS

2.1 Tonle Sap Lake

Modulated by monsoon systems, the Mekong's hydrology has distinct wet and dry season features (Chen, Chen, & Azorin-Molina, 2018; Delgado, Merz, & Apel, 2012; MRC, 2010b). Linking to the Mekong mainstream, the TSL is governed by the hydraulic gradient between the mainstream and TSL, causing a reverse flow of Tonle Sap River in wet seasons (MRC, 2010a). The reverse flow from the Mekong into the TSL usually starts in May and ends in September (Kummu et al., 2014; MRC, 2019; Uk et al., 2018), contributing to more than 50% of the TSL's annual volume change (Kummu et al., 2014). The lake's water level ranges between ~1 and ~10 meters above the mean sea level (m), driving the inundated floodplain fluctuating between ~2,500 km² and ~15,000 km². The data and methods are described in detail as follows.

2.2 Tonle Sap Lake water level and inundation area

Daily water level data of Kompong Luong (WL_{KL} at the lake), Prek Kdam (WL_{PK} at the Tonle Sap River), and Phnom Penh port (WL_{PPP}) (see Figure 1) were collected from the Mekong River

Commission (<http://www.mrcmekong.org/>). WL_{KL} was available from 01 January 1997 to 30 September 2020, whereas WL_{PK} and WL_{PPP} were available from 01 January 1960 to 30 September 2020. Since water levels in the TSL and Tonle Sap River are strongly correlated (cf. Arias et al. (2013) and Inomata and Fukami (2008)), we first used multiple polynomial regression to predict WL_{KL} with WL_{PK} and the difference between WL_{PK} and WL_{PPP} for the period 1997 – 2020 (see Eq. (1-2)), in which 80% of the data were used for training and the rest were for testing. When comparing the observations against modeled WL_{KL} on the test set of data, the estimated time series showed a Nash-Sutcliffe efficiency of 0.97 and a Root-mean-square error of 0.47 m, indicating thus a good fit with the data (Figure 2). A complete series of daily WL_{KL} was then estimated using multiple polynomial regression from 01 January 1960 to 30 September 2020 (Figure S1). In this study, we focused on the hydrological year (1 May – 30 April) and divided it to wet season (May – October) and dry season (November – April) to be consistent with the flood timing (Kummu & Sarkkula, 2008).

$$WL_{KL} \sim \text{polym}(\text{Diff}_{PPP-PK}, WL_{PK}, \text{degree} = 3, \text{raw} = \text{TRUE}) \quad \text{Eq. (1)}$$

$$\text{Diff}_{PPP-PK} = WL_{PPP} - WL_{PK} \quad \text{Eq. (2)}$$

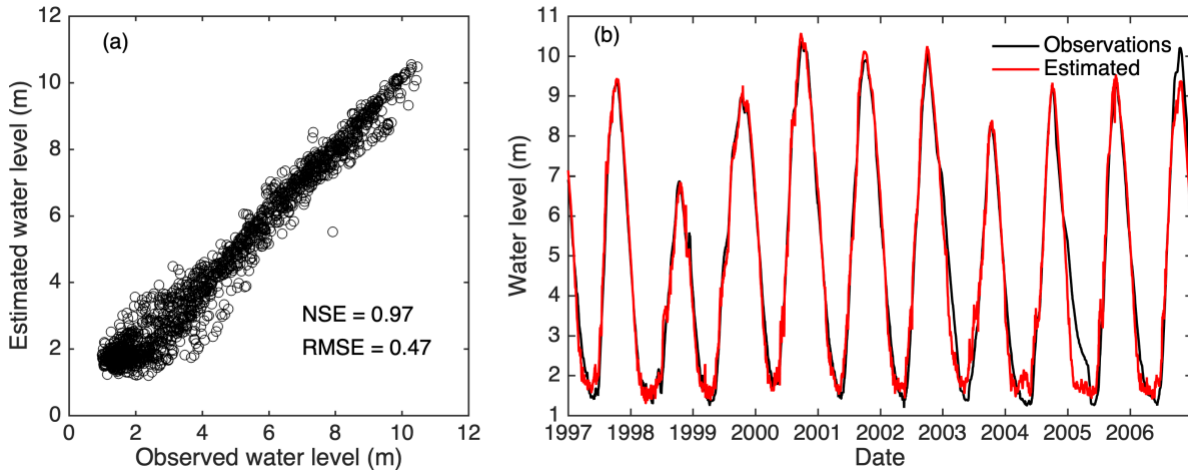


Figure 2. Comparison of the observed water level at Kompong Luong (WL_{KL}) station and estimated water level based on multiple polynomial regression (a) on the test set of data for 1997 – 2020 and (b) for 1997 – 2006. The estimated time series had a Nash-Sutcliffe efficiency (NSE) of 0.97 and a Root-mean-square error (RMSE) of 0.47 m, indicating a good fit with the observed data.

To estimate the daily inundation area and lake volume, we employed a Digital Bathymetry Model of the TSL using WL_{KL} , following the method from Kummu & Sarkkula (2008) and Kummu et al. (2014), which has also been applied by Arias et al. (2013). Good agreements of water level and surface extent between this method and a MODerate resolution Imaging Sensor (MODIS)-based estimation demonstrate the accuracy of this method (Frappart et al., 2018). Hence, daily inundation area and lake volume data throughout 1960 – 2019 were obtained. Regarding the flood pulse change, we assessed the changes in the key flood pulse parameters (Junk et al., 1989; Kummu, Keskinen, & Varis, 2008; Lamberts, 2006) as shown in Table 1.

Table 1. Definition of key flood pulse parameters for each hydrological year from 1 May – 30 April

Flood pulse parameter	Acronym	Definition
Annual water level	WL_hy	Annual mean water level (1 May – 30 April)
Wet season water level	WL_wet	Wet season mean water level (1 May – 31 October)
Dry season water level	WL_dry	Dry season mean water level (1 November – 30 April)
Maximum water level	WL_max	Maximum daily water level defined as the 95 th percentile for daily water level
Minimum water level	WL_min	Minimum daily water level defined as the 5 th percentile for daily water level
Water level amplitude	WL_amp	The amplitude of water level between WL_max and WL_min
Flooded area amplitude	WA_amp	The amplitude of inundation area between maximum and minimum flooded area (defined as the 95 th and 5 th percentile for daily inundation area, respectively)
Start date of a flood	StartDate_Flood	Start date of a flood when the water level is above 2 m for the first time
End date of a flood	EndDate_Flood	End date of a flood when the water level is below 2 m for the first time after the start date of the flood
Flood duration	Duration_Flood	Duration of a flood is the days between StartDate_Flood and EndDate_Flood
Date of WL_max	WL_max_date	The date when WL_max occurs defined as the intermediate date when the water level is greater than the WL_max
Date of WL_min	WL_min_date	The date when WL_min occurs defined as the intermediate date when the water level is lower than the WL_min

2.3 Atmospheric circulations indices

As climate influences the hydrology in the MRB and flood regime of the TSL (Kummu et al., 2014), large-scale atmospheric circulation index data were also employed, including El Niño-Southern Oscillation (ENSO), Pacific Decadal Oscillation (PDO), and Indian Ocean Dipole (IOD). They have strong connections to the hydroclimate in the MRB (Delgado, Apel, & Merz, 2010; Hrudya, Varikoden, & Vishnu, 2021; Räsänen & Kummu, 2013). The data for these three indices are available from ESRL/NOAA (https://www.esrl.noaa.gov/psd/gcos_wgsp/Timeseries/): for ENSO data we used NINO 3.4, available from 1870 to present; for PDO it is available from 1900 to present; and for IOD we used the Dipole Mode Index that is available from 1870 to present. We calculated the averaged monthly NINO 3.4 from December to the following February as the annual ENSO index (Chen, Ho, Chen, & Azorin-Molina, 2019); the averaged monthly PDO from November to the following March as the annual PDO index (Feng, Wang, & Chen, 2014); and the averaged monthly IOD from June to November as the annual IOD index (Feng & Chen, 2014).

2.4 Quantification of the temporal changes of the flood pulse parameters

To investigate the flood pulse change in the TSL, we estimated the trend and variability of the lake's flood regime by hydrological year, and by wet and dry seasons. Mann-Kendall (Kendall, 1938) and Sen's slope (Sen, 1968) were employed to estimate the trends, which are widely used in hydroclimate studies (Chen et al., 2018; Wu, Wang, Cai, & Li, 2016; Xue, Liu, & Ge, 2011). Averaged subdecadal variance of the time series (variance of scales lower than 10 years) was also evaluated using the wavelet analysis, which is a commonly used tool for analyzing the time-space frequencies of non-stationarity hydroclimate time series (Delgado et al., 2012; Taleb & Druryan, 2003; Torrence & Compo, 1998), using a toolkit from Torrence & Compo (1998). The R package 'segmented' based on regression models was used to detect breakpoints of the interannual time series (Muggeo, 2003, 2017), which can compute the optimal breakpoints (Ferguson, Humphry, Lawson, Brendel, & Bechtold, 2018).

To measure shift days of the daily water level before and after the detected breakpoints (in 1986 and 2000 estimated in this study), we first calculated the mean daily water level for the two periods (i.e., 1986 – 2000 and 2000 – 2019) and divided the hydrograph into two time periods at the joint. Then the mean difference of the shift days between the two periods was calculated separately. We measured the return periods of the inundation area in the three time periods divided by the breakpoints using the Gumbel distribution. The Pearson correlation coefficient was used to quantify correlations between the flood pulse parameters and large-scale atmospheric circulations (ENSO, PDO, and IOD). Using a 21-year moving window, we analyzed the changes in correlation between the flood pulse parameters (i.e., water level) and the atmospheric circulations for 1960 – 2019.

2.5 Anthropogenic impacts on flood pulse

Owing to the complex TSL system and lacking observations, it is difficult to quantify the human activity impacts on the flood pulse with available data. Considering the rapid increasing dams in the upper stream of the lake, primarily shifting the seasonal flow regime (Hecht et al., 2019; Yun et al., 2020), seasonal change of discharge in the upstream Stung Treng station (a station with long observations close to the lake, see Figure 1) could reflect the potential impacts on flood pulse from the hydropower development. Following Kallio & Kummu (2021), we employed the following discharge data to measure the trend of high flow (Q5) and low flow (Q95):

- observed discharges in the Stung Treng station for 1960 – 2019, including both climatic and anthropogenic impacts, and;
- simulated discharges from GLOFAS global streamflow reanalysis products from 1979 without the information of the recent hydropower development and thus reflecting only the climatic impacts on discharges (Alfieri et al., 2020; Kallio & Kummu, 2021).

We were then able to disentangle the climatic and anthropogenic impacts on changes in discharge in Stung Treng by comparing the difference between the observed and simulated data.

3. RESULTS

3.1 Changes in flood pulse parameters

Changes in the flood pulse parameters are shown in Figures 3 – 5 and summarized in Table 2. The annual mean water level (WL_hy) of the TSL has fluctuated between 1960 and 2019 (Figure 3a). The lowest WL_hy can be seen in dry years 1998, 2010, and 2015, and the highest WL_hy in wet years 1996, 2000, and 2011. Breakpoints were found in 1986 and 2000; the 11-year moving average of WL_hy rose between 1986 and 2000 ($p < 0.01$) and fell significantly in the other two periods (1960 – 1986 and 2000 – 2019) (see Table 2). Time series of the averaged wet season water level (WL_wet) also fluctuated over the years, however no breakpoint was detected (Figure 3b). The averaged dry season water level (WL_dry) rose during 1986 and 1996 ($p < 0.001$) and decreased significantly at the other two time periods (1960 – 1986 and 1996 – 2019) (Figure 3c). WL_hy had significant subdecadal variability in the 1990s and 2010s, whereas such variability for WL_wet was significant in the 1970s – 2010s. In addition, all the three parameters showed increasing subdecadal variabilities before the 2000s. Overall, these results indicate clear rising and falling stages of the water level over 1960 – 2019, with significant subdecadal variability; and there were apparent declining trends of WL_hy and WL_dry from the late 1990s. Similar results could also be found for the inundation area and water volume (Figure S2 –S3).

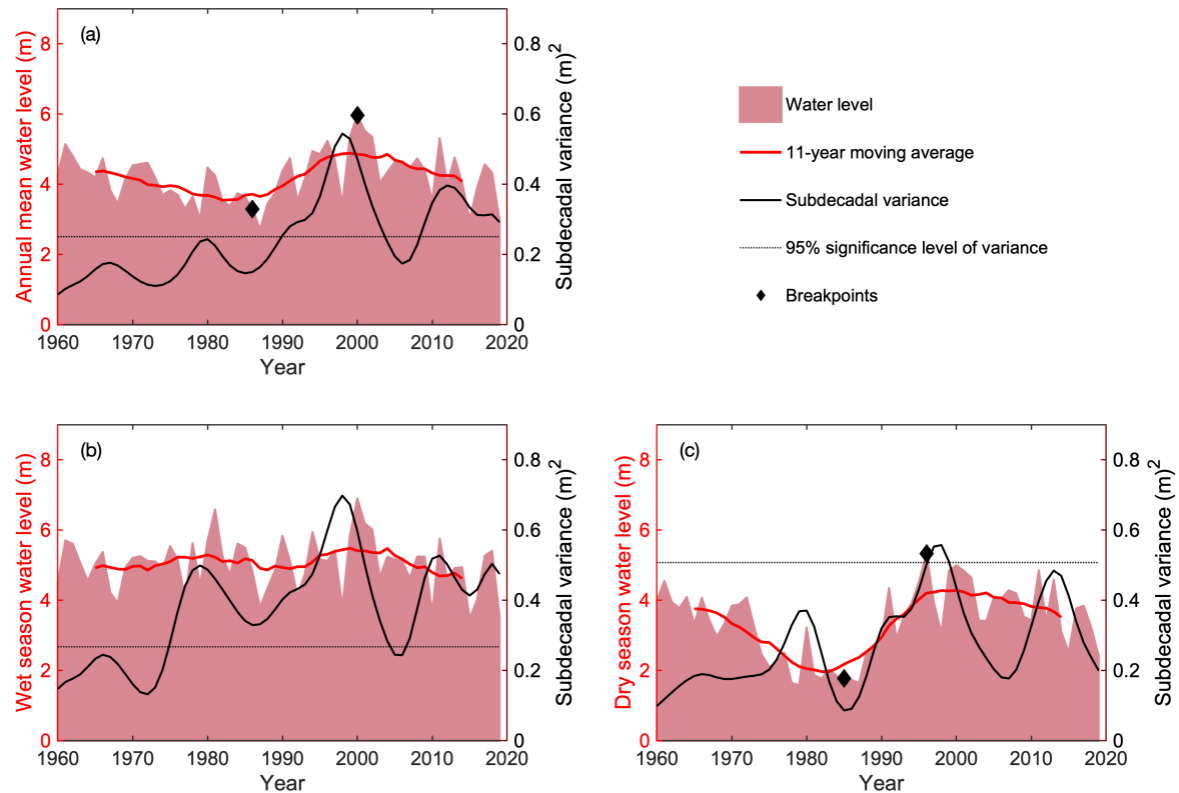


Figure 3. Time series of water level of the Tonle Sap Lake for 1960 – 2019: Mean water level: (a) annual, (b) wet season (May – October), and (c) dry season (November – April). The red line is the 11-year moving average of water level time series, whereas the black line represents the subdecadal variance (variance of scales lower than 10 years) of the water level estimated by wavelet analysis, with significance level of 95% shown in black dash line. The breakpoints are marked with diamond markers determined with R package ‘segmented’ (Muggeo, 2003, 2017).

Interannual changes of the TSL’s peak water level and inundation area for 1960 – 2019 are displayed in Figure 4a-c. The annual WL_max fluctuated between 6 and 11 m, with a significant subdecadal variability from the mid-1980s. The WL_max has two breakpoints in 1988 and 2001 and it significantly decreased from 2001 (-0.14 m/year, $p < 0.05$). The annual WL_min displayed an increasing trend before the breakpoint in 2003 (0.005 m/year, $p < 0.01$) with no significant trend after that. It has significant subdecadal variability from the 1990s. Several spikes in the peak water level revealed large flood and drought events (i.e., 1996, 1998, 2000). The amplitude between WL_max and WL_min (WL_amp) followed a similar trend with the WL_max, as

WL_min has stayed rather stable (Figure 4c). The amplitude between maximum and minimum inundation area also showed a similar trend with the WL_max and WL_amp (Figure 4d). Besides, these parameters showed increasing subdecadal variabilities from the 1960s.

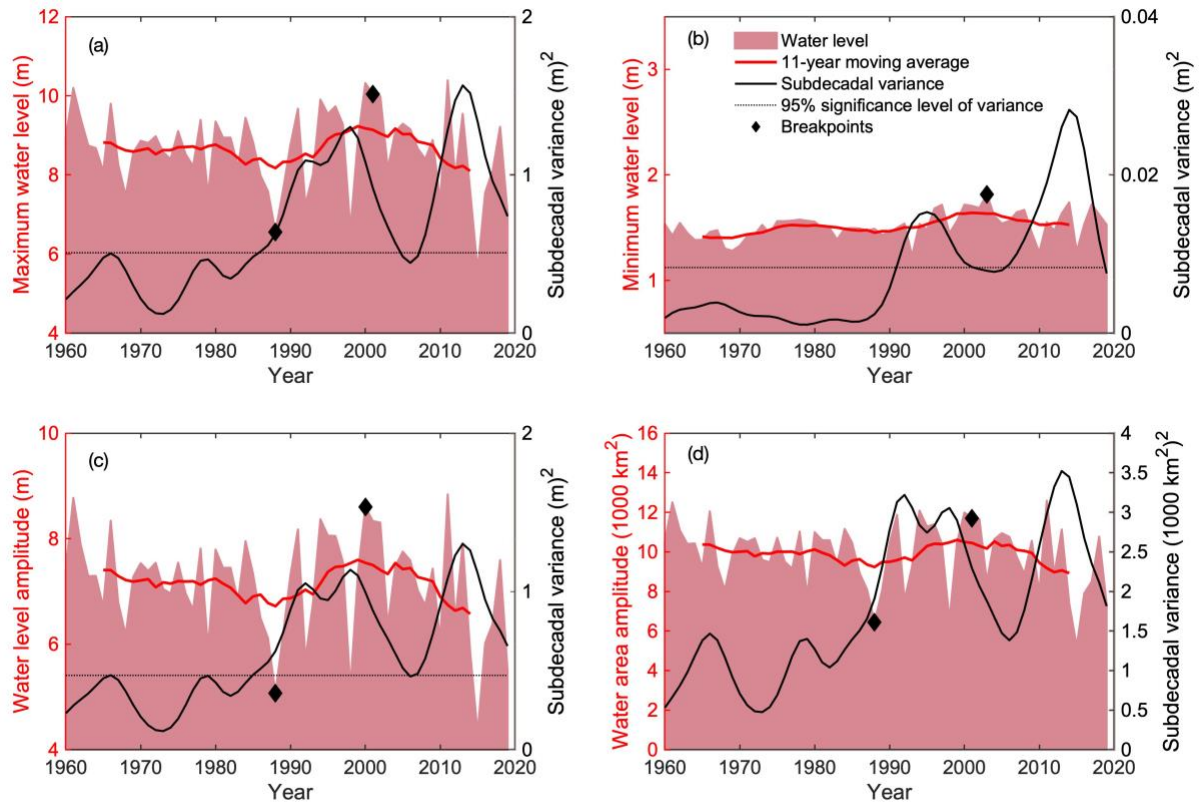


Figure 4. Time series of the Tonle Sap Lake's peak water levels and inundation area for 1960 – 2019. The maximum (a) and minimum (b) is defined as the 95th- and 5th- percentile of the daily water level records over hydrological year, with the difference between the maximum and minimum water levels defining the water level amplitude (c), and water area amplitude (d). The red line is the 11-year moving average of water level time series, whereas the black line represents the subdecadal variance (variance of scales lower than 10 years) of the water level estimated by wavelet analysis, with significance level of 95% shown in black dash line. The breakpoints are marked with diamond markers determined with R package 'segmented' (Muggeo, 2003, 2017).

The StartDate_Flood, EndDate_Flood, Duration_Flood, WL_max_date, and WL_min_date fluctuated over 1960 – 2019 (Figure 5 and Table 2). Both StartDate_Flood and WL_min_date

had a breakpoint around 2000; however, they significantly delayed and advanced after 2000, respectively ($p < 0.05$). The WL_max_date and Duration_Flood both had two breakpoints around 1981 – 1984 and 1993 – 1994; and they both decreased before the first breakpoint ($p < 0.01$), with no significant trend after the second breakpoint. The EndDate_Flood had a breakpoint in 1986 that advanced (-3.96 day/year, $p < 0.001$) and delayed (1.47 day/year, $p < 0.01$) before and after the breakpoint, respectively. Similar to the WL_wet, the StartDate_Flood had significant subdecadal variability from the mid-1970s. The EndDate_Flood and Duration_Floods both have significant variability in the 1970s. And the WL_max_date and WL_min_date had significant variabilities in the 1970s – 1980s and 1970s – 2010s, respectively. Overall, these results indicate an exceptionally high subdecadal variability in the lake's flood between the 1970s and 1990s; the StartDate_Flood, EndDate_Flood, and the WL_max_date have delayed from 2000, 1986, and 1981, respectively.

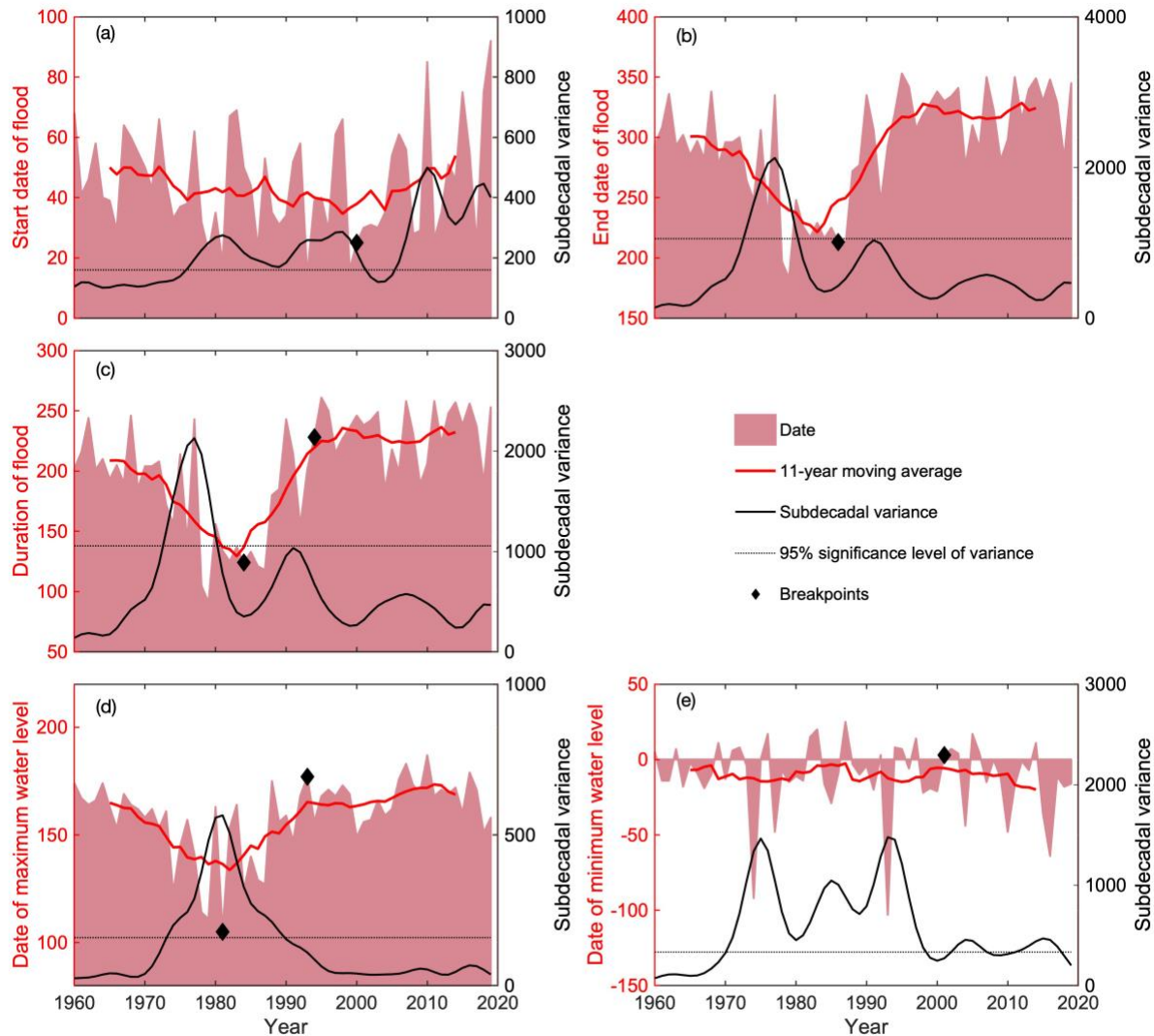


Figure 5. Time series of the Tonle Sap Lake's flood timing for 1960 – 2019. The start and end dates of a flood are defined as the dates when the water level is above and below 2 m water level for the first time, respectively (Kummu et al., 2008). The dates of maximum and minimum water levels are the intermediate dates when the water level is greater and lower than the maximum and minimum water levels, respectively. The red line is the 11-year moving average of the flood time series, whereas the black line represents the subdecadal variance (variance of scales lower than 10 years) of the flood timing estimated by wavelet analysis, with significance level of 95% shown in black dash line. The breakpoints are marked with diamond markers determined with R package 'segmented' (Muggeo, 2003, 2017). In this study, we focused on the hydrological year (1 May – 30 April), so that the 1st of May is numbered as 0 and dates before that are negative.

294 Table 2. Summary of changes in flood pulse parameters. Breakpoints were determined with R package ‘segmented’
295 based on regression models (Muggeo, 2003, 2017). Subdecadal variability was assessed with wavelet analysis
296 (Torrence and Compo, 1998; Taleb and Druyan, 2003; Delgado *et al.*, 2012). Trends were estimated with Mann-
297 Kendall (Kendall, 1938) and Sen’s slope (Sen, 1968) method.

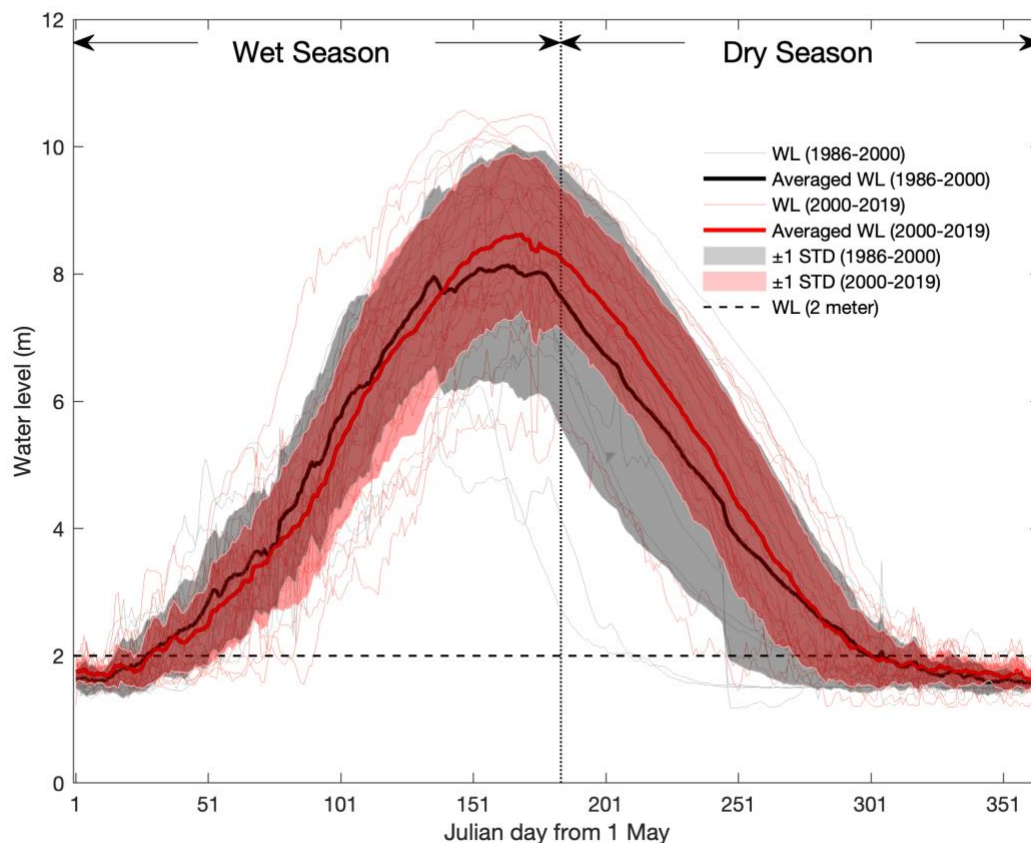
Flood pulse parameter	Time periods delineated by breaks	Trend in mean (m/year or days/year)	Trend in subdecadal variability ([m]²/year or [km²]²/year)
Annual water level (WL_hy)	1960 – 1986	-0.05***	0.003*
	1986 – 2000	0.17**	0.03***
	2000 – 2019	-0.08**	-0.0006
Wet season water level (WL_wet)	1960 – 2019	-0.002	0.005***
Dry season water level (WL_dry)	1960 – 1986	-0.10***	0.004*
	1986 – 1996	0.32***	0.03***
	1996 – 2019	-0.07**	-0.008
Maximum water level (WL_max)	1960 – 1988	-0.03	0.008***
	1988 – 2001	0.16**	0.04*
	2001 – 2019	-0.14*	0.03
Minimum water level (WL_min)	1960 – 2003	0.005**	0.0001
	2003 – 2019	-0.003	0.001*
Water level amplitude (WL_amp)	1960 – 1988	-0.03	0.008*
	1988 – 2000	0.13	0.03*
	2000 – 2019	-0.13**	0.011
Flooded area amplitude (WA_amp)	1960 – 1988	-57.8	26'353*
	1988 – 2001	201.8	-1'356
	2001 – 2019	-204.2*	52'158
Start date of a flood (StartDate_Flood)	1960 – 2000	-0.39	4.43***
	2000 – 2019	1.76*	16.95***
End date of a flood (EndDate_Flood)	1960 – 1986	-3.96***	36.19
	1986 – 2019	1.47**	-9.25*
Flood duration (Duration_Flood)	1960 – 1984	-4.00**	53.53**
	1984 – 1994	10.44**	74.88**
	1994 – 2019	0.13	-2.19
Date of WL_max (WL_max_date)	1960 – 1981	-2.00**	22.61***
	1981 – 1993	4.00*	-29.02***
	1993 – 2019	0.09	-0.04
Date of WL_min (WL_min_date)	1960 – 2001	-0.43	22.25
	2001 – 2019	-1.35***	-0.05

*, $p < 0.05$; **, $p < 0.01$; ***, $p < 0.001$

299

300 3.2 Changes in the hydrograph

301 The years of 1986 and 2000 appeared as breakpoints in many of the above-analyzed flood pulse
 302 parameters (Figures 3-5, Table 2), and flood timing displayed a trend of advancement before
 303 1986 and delay after 2000. Figure 6 presents a hydrograph of mean daily water level for the two
 304 periods of 1986 – 2000 and 2000 – 2019. Compared to the former period, our results show that
 305 the flood regime was delayed in 2000 – 2019. The average of such delays was about 4.7 and 10.0
 306 days in the wet and dry seasons, respectively.



307

308 **Figure 6.** Hydrograph of the Tonle Sap Lake for 1986 – 2000 and 2000 – 2019. The STD refers
 309 here to standard deviation, and the gray and red shading represent the ± 1 standard deviation of
 310 the daily mean water level. The gray (red) lines represent the daily water level in the years for
 311 1986 – 2000 (2000 – 2019), with the thick black (red) line represents the mean of the daily mean
 312 water level.

3.3 Changes in return period of flood inundation area

Figure 7 shows the high and low inundation area (i.e., 1-month and 11-month inundation areas) of the TSL floodplain at different return periods in 1960 – 1986, 1986 – 2000, and 2000 – 2019. Regarding the return period of 1-month inundation area, 1986 – 2000 witnessed the largest inundation area at all return periods, followed by 2000 – 2019 and 1960 – 1986. For example, a 100-year return period event of inundation was about 15,753 km²; this value increased to 19,408 km² in 1986 – 2000 and decreased to 18,234 km² in 2000 – 2019 (Figure 7a). In terms of the low inundation area, similar results occurred with increased inundation areas for the latter two periods (Figure 7b). However, 2000 – 2019 had a slightly larger inundation area than that of 1986 – 2000 at the same return periods. Overall, these results indicate consistent rising probabilities of low inundation area in the TSL in 2000 – 2019, and the declining probabilities of high inundation area in 2000 – 2019 compared to 1986 – 2000 suggest an increasing probability of shrinking lake area.

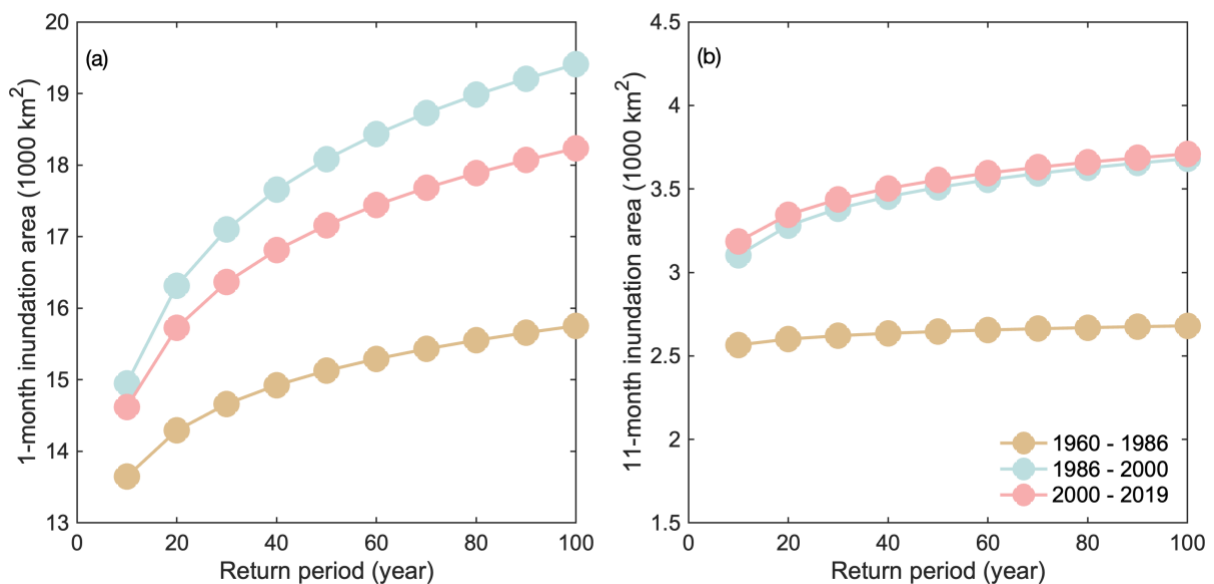


Figure 7. Comparing the inundation area of the Tonle Sap Lake at different return periods in 1960 – 1986, 1986 – 2000, and 2000 – 2019. 1-month inundation area represents high inundation area in the wet season, and 11-month inundation area represents low flood inundation area in the dry season. The return period of the inundation area was estimated using the Gumbel distribution.

3.4 Correlation with atmospheric circulation indices

Correlations between the large-scale atmospheric circulations (Figure S4) and flood pulse parameters are displayed in Table 3. Both ENSO and PDO had significant negative correlations with the water level at annual and wet season scales, together with peak water level and area (WL_max, WL_amp, and WA_amp). The ENSO and PDO also strongly correlated with the StartDate_Flood and WL_dry, respectively, and the IOD showed a significant positive correlation with the StartDate_Flood.

Table 3. Correlation coefficients between key flood pulse parameters and large-scale atmospheric circulations: El Niño-Southern Oscillation (ENSO), Pacific Decadal Oscillation (PDO), and Indian Ocean Dipole (IOD).

Flood pulse parameter	ENSO	PDO	IOD
Annual water level (WL_hy)	-0.36**	-0.41**	0.07
Wet season water level (WL_wet)	-0.48***	-0.31*	0.00
Dry season water level (WL_dry)	-0.16	-0.35**	0.10
Maximum water level (WL_max)	-0.35**	-0.36**	0.06
Minimum water level (WL_min)	-0.22	0.06	0.15
Water level amplitude (WL_amp)	-0.33**	-0.39**	0.04
Flooded area amplitude (WA_amp)	-0.32*	-0.38**	0.04
Start date of a flood (StartDate_Flood)	0.39**	0.19	0.27*
End date of a flood (EndDate_Flood)	-0.02	-0.13	0.18
Flood duration (Duration_Flood)	-0.02	-0.13	0.18
Date of WL_max (WL_max_date)	0.17	-0.08	0.10
Date of WL_min (WL_min_date)	-0.01	-0.10	0.20

*, $p < 0.05$; **, $p < 0.01$; ***, $p < 0.001$

Taking WL_wet as an example, Figure 8 presents changing correlations between the WL_wet and atmospheric circulations using a 21-year moving window for 1960 – 2019. The WL_wet had a negative correlation coefficient with ENSO, which increased over time and became significant since the 1990s, indicating potential associations between ENSO and water level. This also

means that the correlation between ENSO and water level is changing over time. The WL_wet negatively correlated with PDO, and the coefficient was significant in the 1990s and late 2000s. As to WL_wet and IOD, they shifted from negative correlation to positive correlation but remained insignificant over the whole period. The significant correlations between WL_wet and ENSO and PDO coincide with the wave pattern of WL_wet's subdecadal variance, especially in the mid-1970s, 1990s, and late 2000s (see Figure 3). The breakpoints around 1986 and 2000 concurred with the timing of significant correlations between them, indicating strong associations between the lake's flood regime and atmospheric circulations, ENSO and PDO in particular. In addition, we found significant wavelet coherence changes between WL_wet and atmospheric circulations at the frequency of two- to fourteen-year periods; and the anti-phase between them indicates that the wet years tend to be associated with cold events (Figure S5). Overall, our results suggest that the large-scale atmospheric circulations could have influenced the water level of the TSL in different time scales.

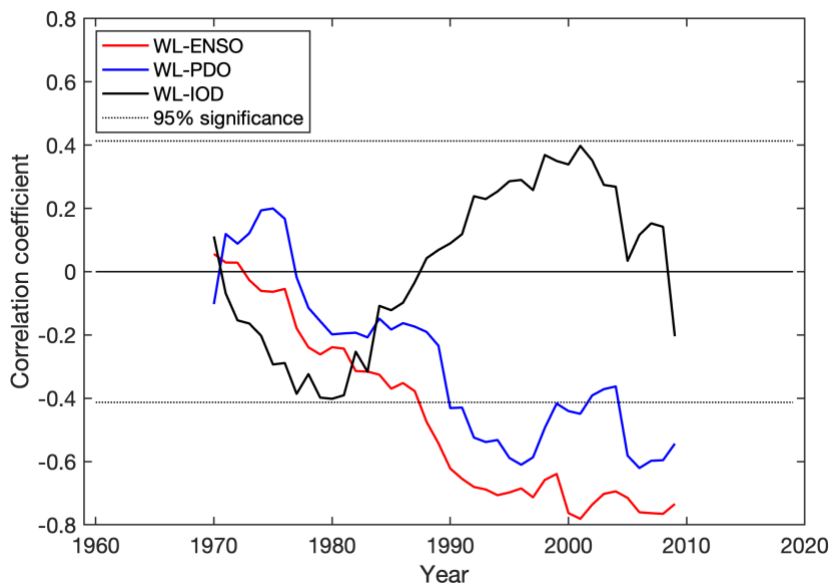


Figure 8. 21-year moving window correlation between the averaged wet season water level and atmospheric circulations, as an example correlation. See tabulated results in Table 3. The value of a 21-moving window is marked using the year in the middle. For example, for the correlation coefficient in 1970, it represents the correlation between 1960 and 1980. ENSO stands for El Niño-Southern Oscillation, PDO for Pacific Decadal Oscillation, and IOD for Indian Ocean Dipole. See the oscillation indices for 1960-2019 in Supplementary Figure S4.

3.5 Anthropogenic impacts on the flood pulse

To understand the anthropogenic impacts on the Tonle Sap flood pulse, we used the observed and modeled discharges in the Mekong mainstream in Stung Treng as a proxy (Figure 9). Given the two breakpoints in 1986 and 2000 of the flood pulse parameters (i.e., WL_hy, WL_dry, EndDate_Flood, see Figures 3-5 and Table 2), we compared the linear trend lines of 1986 – 2000 and 2000 – 2019 for low and high water levels in the lake (Figure 9a,b) with those for low and high discharges (Figure 9c-f). We found that the apparent shifts in observed low TSL water levels between the two periods are not shown in the observed low discharges in Stung Treng (Figure 9a,c). While simulated low discharges with climatic impacts only showed no trend in either of the two periods (Figure 9e), the observed low flows (with dam operations included) showed a clear upward trend since the 1990s. This indicates that the increased low season discharges are due to anthropogenic drivers but are not shown in the water levels in the lake. On the contrary to this, the high water levels in TSL show a similar trend to the observed high discharges (Figure 9b,d): upward trend until the year 2000 and then sharply decreasing trend. In simulated high discharges, this is not visible (Figure 9f), indicating that anthropogenic drivers have influenced the high discharges in Stung Treng and also the changes in high water levels, and thus some flood pulse parameters, in the TSL.

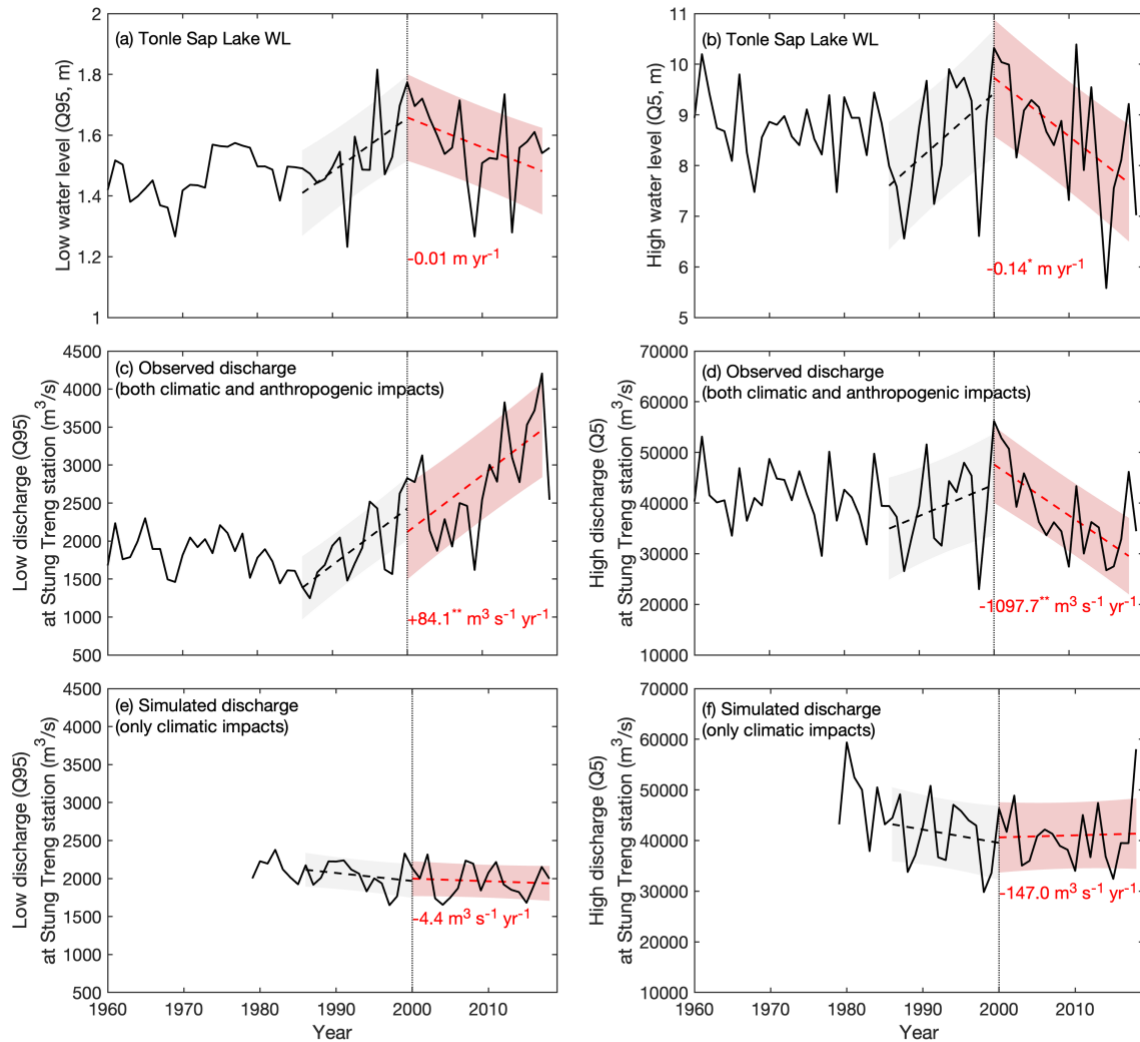


Figure 9. Trend analysis of water level of the Tonle Sap Lake and discharges at Stung Treng station. Low (Q95, a) and high (Q5, b) water level of the Tonle Sap Lake; Low (Q95) and high (Q5) observed discharge at Stung Treng station, including both climatic and anthropogenic impacts on discharge (c, d) and simulated discharge from GLOFAS model, including only climatic impacts on discharge (e, f). Given the two breakpoints in 1986 and 2000 of the flood pulse parameters (see Figure 3-5 and Table 2), we assessed the linear trend lines of 1986 – 2000 (black dash line) and 2000 – 2019 (red dash line) for the low and high water levels as well as the observed and simulated discharges. The gray and red shading represent the ± 1 standard deviation of the regression. The value of the trend of 2000 – 2019 is shown in red text in each subfigure.

4. DISCUSSION

4.1 Flood pulse change in the Tonle Sap Lake

This study showed significant decreasing trends of water levels and inundation areas from the late 1990s in the dry season and annual scales (Figure 3). This is in line with previous studies (Kallio & Kummu, 2021; Lin & Qi, 2017; Wang et al., 2020; Wang, Feng, Liu, & Chen, 2021), indicating a substantially diminished flood pulse of the TSL from 2000. Existing literature based on remote sensing data and other resources have limited with the available time series of water level and inundation area data from the late 1980s (Dang et al., 2016; Ji et al., 2018; Sakamoto et al., 2007; Tangdamrongsub et al., 2016), but our study provides a more extended time period analysis and puts the flood pulse change to the TSL since the late 1990s into a longer time perspective. Numerous studies exist on the impacts of hydropower development on the flood pulse of the TSL and to the changes in the higher (lower) dry (wet) season water levels (Arias et al., 2012; Kallio & Kummu, 2021; Keskinen, Someth, Salmivaara, & Kummu, 2015; Kummu & Sarkkula, 2008). Our results revealed that, indeed, the maximum water level and inundation area had decreased significantly since 2000, but no trend was found for the minimum water level (Table 2, Figure 9). Cochrane et al. (2014) and Ji et al. (2018) compared two time periods (before and after 1991 [1960 – 2010] and 2008 [2000 – 2014], respectively) also found diminishing flood pulse; and Ji et al. (2018) showed decreasing dry season inundation area. Our study based on the long term daily water level revealed a more worrisome situation of the diminishing flood pulse of the TSL at annual and dry season scales than previous studies suggested (Table 2), accompanied by the increasing subdecadal variability, which strongly connects to the livelihood of the local residents.

The lake has experienced interannual fluctuations of water level, inundation area, and water volume throughout the observed period from 1960, accompanied by significant subdecadal variabilities from the 1980s. The increasing variance of lake's water level could be compared and validated with precipitation and discharge data (Delgado et al., 2010; Ho, Baik, Kim, Gong, & Sui, 2004; Wang, Wu, & Lau, 2001). Many studies have presented evidence of the impacts of climate change on the changes in Mekong flow and TSL (Day et al., 2011; Delgado et al., 2012; Frappart et al., 2018; Lauri et al., 2012; Räsänen & Kummu, 2013; Wang et al., 2021). There are

strong connections between atmospheric circulations and hydrology at the southern MRB (Delgado et al., 2012; Räsänen & Kummu, 2013; Ruiz-Barradas & Nigam, 2018; Xue et al., 2011). Moreover, Frappart et al. (2018) found significant correlations between the lake's surface water volume and rainy season rainfall in the MRB, and the TSL's hydroclimatic extremes had a strong connection to the large-scale atmospheric circulations; Wang et al. (2020, 2021) also revealed significant correlations between the lake's inundations and precipitation in the region north of the TSL at annual and seasonal scales. Therefore, the basin-wide and lake's hydrological changes highly correlated with the large-scale climate (Delgado et al., 2012; Frappart et al., 2018). Our results of the significant correlation between water level and atmospheric circulations (ENSO, PDO, and IOD) using the 21-year moving window from the 1980s indicated strong connections between the high variability of flood pulse and atmospheric circulations over the period (Figure 8, Table 3). And their significant coherence variances (Figure S5) also indicate that atmospheric circulations could have strongly influenced the flood pulse of the TSL in different time scales.

Impacts of hydropower have been the main focus in many recent investigations (Arias, Piman, Lauri, Cochrane, & Kummu, 2014; Cochrane et al., 2014; Hecht et al., 2019; Ji et al., 2018; Kallio & Kummu, 2021; Lin & Qi, 2017; Räsänen, Koponen, Lauri, & Kummu, 2012; Räsänen et al., 2017; Wang et al., 2021). The apparent differences in the trend between the observed and simulated discharges at Stung Treng station (Figure 9) suggested the potential impacts of hydropower development on discharges in the Mekong mainstream and flood pulse parameters in the TSL. Kallio & Kummu (2021) also showed that all major dams in the Mekong Basin are critical in recent impacts on the flood pulse change. Future simulations with combined scenarios of hydropower and climate change are projected to impact, e.g., the inundation area, gallery forest, and sediments, indicating degrading ecosystem services of the TSL in the future (Arias, Cochrane, et al., 2014). Furthermore, future flow regime in the Mekong is projected to be driven by the planned hydropower development (Anh, Hoang, Bui, & Rutschmann, 2019; Arias et al., 2012; Dang et al., 2016; Lauri et al., 2012; Räsänen et al., 2012) and climate change (Delgado, Merz, & Apel, 2014; Hoang et al., 2016; Keskinen et al., 2010; Kingston, Thompson, & Kite, 2011; Yun et al., 2021). Considering the crucial role of the flood pulse of the TSL on the

livelihood and biodiversity in Cambodia and the Mekong region, any changes to the flood pulse could be devastating to the regional sustainability (Lamberts, 2006; Uk et al., 2018).

4.2 Potential impacts of the flood pulse change on fishery

The flood regime of the TSL is critical to the fishery, including the magnitude, timing, and variations (Arias et al., 2013; Baran, 2006; Day et al., 2011; Poulsen et al., 2002). For instance, high water levels are more favorable to the breeding and dispersal of fish larvae, and variation of water levels is a critical fish migration trigger (Baran, 2006; MRC, 2010a) because higher floods cultivate higher fish yield (MRC, 2010a). However, the elevated water level variance could interrupt the fish migration and disturb the fish production, which is the primary protein source in the region (Keskinen, 2006; Lamberts, 2006; Uk et al., 2018). Previous studies have found drops of fish catches and fish size in the TSL for 2000 – 2015 (Ngor et al., 2018) and 1994 – 2000 (Chan, Ngor, So, & Lek, 2017), respectively. Moreover, our results indicate substantial flood pulse shifts for about 5 and 10 days in the wet and dry seasons in 1960 – 1986 and 2000 – 2019, respectively (Figure 6). Such shift could directly affect the migratory fish (Baran, 2006; MRC, 2010a). However, there is still a lack of knowledge of the impacts of flood regime changes on the fishery (Lamberts, 2006; Uk et al., 2018), requiring more endeavor to better understand water and fishery management.

Flood pulse change could further influence the socio-economic system in the TSL. Combined with the diminishing flood pulse, population booming in Cambodia and TSL floodplain areas since the 1980s has exacerbated the crop production expansion and indiscriminate fishery (Kc et al., 2017; Ngor et al., 2018; Salmivaara et al., 2016). Furthermore, increased water level variability has caused an unstable cropping system and posed environmental shocks on farmers (Heinonen, 2006). Along with the deteriorating fishery (Chan et al., 2017; Ngor et al., 2018), people's occupations have witnessed a shift from fishery to other occupations, such as forestry and hunting (National Institute of Statistics, 2018). Owing to the improving livelihood opportunities in urban areas, e.g., Phnom Penh and Thai cities, many farmers have migrated to other areas as a replacement for local livelihood strategies since the late 1990s (Bylander, 2015;

Heinonen, 2006). Overall, the flood pulse change could hamper the socio-economic development of the TSL area.

4.3 Limitations and way forward

In terms of the data used, uncertainties of this study arise from the estimated time series of water level using the multiple polynomial regression due to the lacking observed time series for the whole study period, as well as assessing the inundation area based on the Digital Bathymetry Model. The comparisons between the existing observations and our modeled water level have shown a good fit of the data, suggesting that the estimated time series could reflect the flood pulse change reasonably well. Good agreements of water level and surface extent between the method employed in our study and Frappart et al. (2018) based on MODIS estimation also validated our methods in estimating the flood pulse of the TSL.

In terms of estimating the drivers of the changes in flood pulse parameters, we needed to use proxies, including indices on large-scale atmospheric circulations as well as modeled discharge in the Mekong mainstream. While these proxies indicate rather clear messages on the potential impacts of these drivers, future research should focus on to quantitatively assess the impact of all the drivers, such as climatic change, dam construction and operation, human water consumption, land use and land cover change, on different flood pulse parameters. Tools, including basin-wide hydrological models and hydrodynamic models covering the Lower Mekong Floodplains, exist but to apply those for such a long time period would need extensive work on reliable input data, calibration of the models, and then running multiple simulations preferably with multiple models. This information could then be further linked to the ecosystem services and livelihood in the region.

5. CONCLUSIONS

This study has quantified the flood pulse change in the TSL since the 1960s. The results showed decreasing water levels in the dry season and for the whole year since the late 1990s. The mean seasonal cycle of daily water level in the dry and wet seasons for 2000 – 2019, compared to that for 1960 – 1986, have shifted by 10 and 5 days, respectively. Rising probabilities of extreme

inundation area in the later period compared to the earlier period were also identified. The annual flood pulse parameters had strong correlations with the large-scale atmospheric circulations from the 1980s. Moreover, coherence changes between the WL and atmospheric circulations further indicated the influence of atmospheric circulations on the flood pulse in different time scales. Also, apparent differences between the climatic and anthropogenic impacts on the discharge at Stung Treng station in the Mekong mainstream indicate that anthropogenic activity has affected the flood pulse parameters, especially the high water level in the TSL. Our long-term assessment of the changes to the crucial TSL flood pulse could support future research to quantify the impacts of flood pulse change on the fishery and livelihood of the TSL area in Southeast Asia.

ACKNOWLEDGEMENTS

This work was supported by the Strategic Priority Research Program of Chinese Academy of Sciences [XDA20060402, XDA20060401], the China Scholarship Council, the National Natural Science Foundation of China [91537210], and the Swedish STINT [CH2019–8377]. The work is also partly supported by the High-level Special Funding of the Southern University of Science and Technology [Grant No. G02296302, G02296402], Aalto University, Academy of Finland funded project WASCO (Grant No. 305471) and European Research Council (ERC) under the European Union’s Horizon 2020 research and innovation programme (Grant agreement No. 819202).

COMPETING INTERESTS

The authors declare no competing interests.

DATA AVAILABILITY STATEMENT

The data relating to our analyses are available as follows. Water level data is obtained from the Mekong River Commission (<http://www.mrcmekong.org/>), ENSO, PDO, and IOD data is from the Earth System Research Laboratory and NOAA (https://www.esrl.noaa.gov/psd/gcos_wgsp/Timeseries/).

SUPPORTING INFORMATION

Supporting information to this article can be found online at url.

REFERENCES

- Alfieri, L., Lorini, V., Hirpa, F. A., Harrigan, S., Zsoter, E., Prudhomme, C., & Salamon, P. (2020). A global streamflow reanalysis for 1980–2018. *Journal of Hydrology X*, 6, 100049. <https://doi.org/10.1016/j.hydroa.2019.100049>
- Anh, D. T., Hoang, L. P., Bui, M. D., & Rutschmann, P. (2019). Modelling seasonal flows alteration in the Vietnamese Mekong Delta under upstream discharge changes, rainfall changes and sea level rise. *International Journal of River Basin Management*, 17(4), 435–449. <https://doi.org/10.1080/15715124.2018.1505735>
- Arias, M. E., Cochrane, T. A., Kummu, M., Lauri, H., Holtgrieve, G. W., Koponen, J., & Piman, T. (2014). Impacts of hydropower and climate change on drivers of ecological productivity of Southeast Asia ' s most important wetland. *Ecological Modelling*, 272, 252–263. <https://doi.org/10.1016/j.ecolmodel.2013.10.015>
- Arias, M. E., Cochrane, T. A., Norton, D., Killeen, T. J., & Khon, P. (2013). The Flood Pulse as the Underlying Driver of Vegetation in the Largest Wetland and Fishery of the Mekong Basin. *Ambio*, 42, 864–876. <https://doi.org/10.1007/s13280-013-0424-4>
- Arias, M. E., Cochrane, T. A., Piman, T., Kummu, M., Caruso, B. S., & Killeen, T. J. (2012). Quantifying changes in flooding and habitats in the Tonle Sap Lake (Cambodia) caused by water infrastructure development and climate change in the Mekong Basin. *Journal of Environmental Management*, 112, 53–66. <https://doi.org/10.1016/j.jenvman.2012.07.003>
- Arias, M. E., Holtgrieve, G. W., Ngor, P. B., Dang, T. D., & Piman, T. (2019). Maintaining perspective of ongoing environmental change in the Mekong floodplains. *Current Opinion in Environmental Sustainability*, 37(February), 1–7. <https://doi.org/10.1016/j.cosust.2019.01.002>
- Arias, M. E., Piman, T., Lauri, H., Cochrane, T. A., & Kummu, M. (2014). Dams on Mekong tributaries as significant contributors of hydrological alterations to the Tonle Sap Floodplain in Cambodia. *Hydrology and Earth System Sciences*, 18(12), 5303–5315.

<https://doi.org/10.5194/hess-18-5303-2014>

Baran, E. Fish migration triggers in the Lower Mekong Basin and other freshwater tropical systems. MRC Technical Paper No. 14 (2006). Vientiane, Lao PDR. Retrieved from <https://digitalarchive.worldfishcenter.org/handle/20.500.12348/1808>

Bylander, M. (2015). Depending on the Sky: Environmental Distress, Migration, and Coping in Rural Cambodia. *International Migration*, 53(5), 135–147. <https://doi.org/10.1111/imig.12087>

Campbell, I. C., Poole, C., Giesen, W., & Valbo-Jorgensen, J. (2006). Species diversity and ecology of Tonle Sap Great Lake, Cambodia. *Aquatic Sciences*, 68(3), 355–373. <https://doi.org/10.1007/s00027-006-0855-0>

Chadwick, M. T., Juntopas, M., & Sithirith, M. (2008). *Change of Hydrology and Fishery Impacts in the Tonle Sap. The Sustainable Mekong Research Network (Sumernet)*. Bangkok. Retrieved from www.sumernet.org

Chan, B., Ngor, P. B., So, N., & Lek, S. (2017). Spatial and temporal changes in fish yields and fish communities in the largest tropical floodplain lake in Asia. *Annales de Limnologie*, 53, 485–493. <https://doi.org/10.1051/limn/2017027>

Chen, A., Chen, D., & Azorin-Molina, C. (2018). Assessing reliability of precipitation data over the Mekong River Basin: a comparison of ground-based, satellite, and reanalysis datasets. *International Journal of Climatology*, 1–21. <https://doi.org/10.1002/joc.5670>.

Chen, A., Ho, C. H., Chen, D., & Azorin-Molina, C. (2019). Tropical cyclone rainfall in the Mekong River Basin for 1983–2016. *Atmospheric Research*, 66-75. <https://doi.org/10.1016/j.atmosres.2019.04.012>

Cochrane, T. A., Arias, M. E., & Piman, T. (2014). Historical impact of water infrastructure on water levels of the Mekong River and the Tonle Sap system. *Hydrology and Earth System Sciences*, 18(11), 4529–4541. <https://doi.org/10.5194/hess-18-4529-2014>

Dang, T. D., Cochrane, T. A., Arias, M. E., Van, P. D. T., & de Vries, T. T. (2016). Hydrological alterations from water infrastructure development in the Mekong floodplains. *Hydrological Processes*, 30(21), 3824–3838. <https://doi.org/10.1002/hyp.10894>

- 603 Davis, K. F., Yu, K., Rulli, M. C., Pichdara, L., & D’Odorico, P. (2015). Accelerated
604 deforestation driven by large-scale land acquisitions in Cambodia. *Nature Geoscience*,
605 8(10), 772–775. <https://doi.org/10.1038/ngeo2540>
- 606 Day, M. B., Hodell, D. A., Brenner, M., Curtis, J. H., Kamenov, G. D., Guilderson, T. P., ...
607 Kolata, A. L. (2011). Middle to late Holocene initiation of the annual flood pulse in Tonle
608 Sap Lake, Cambodia. *Journal of Paleolimnology*, 45, 85–99.
609 <https://doi.org/10.1007/s10933-010-9482-9>
- 610 Delgado, J. M., Apel, H., & Merz, B. (2010). Flood trends and variability in the Mekong river.
611 *Hydrology and Earth System Sciences*, 14, 407–418. Retrieved from [www.hydrol-earth-](http://www.hydrol-earth-syst-sci.net/14/407/2010/)
612 [syst-sci.net/14/407/2010/](http://www.hydrol-earth-syst-sci.net/14/407/2010/)
- 613 Delgado, J. M., Merz, B., & Apel, H. (2012). A climate-flood link for the lower Mekong River.
614 *Hydrology and Earth System Sciences*, 16(5), 1533–1541. [https://doi.org/10.5194/hess-16-](https://doi.org/10.5194/hess-16-1533-2012)
615 1533-2012
- 616 Delgado, J. M., Merz, B., & Apel, H. (2014). Projecting flood hazard under climate change: An
617 alternative approach to model chains. *Natural Hazards and Earth System Sciences*, 14(6),
618 1579–1589. <https://doi.org/10.5194/nhess-14-1579-2014>
- 619 Feng, J., & Chen, W. (2014). Influence of the IOD on the relationship between El Nino Modoki
620 and the East Asian-western North Pacific summer. *International Journal of Climatology*, 34,
621 1729-1736. <https://doi.org/10.1002/joc.3790>
- 622 Feng, J., Wang, L., & Chen, W. (2014). How does the East Asian Summer Monsoon behave in
623 the decaying phase of El Nino during different PDO phases? *Journal of Climate*, 2682-
624 2698. <https://doi.org/10.1175/JCLI-D-13-00015.1>
- 625 Ferguson, J. N., Humphry, M., Lawson, T., Brendel, O., & Bechtold, U. (2018). Natural
626 variation of life-history traits, water use, and drought responses in Arabidopsis. *Plant*
627 *Direct*, 2, 1–16. <https://doi.org/10.1002/pld3.35>
- 628 Floch, P., & Molle, F. (2009). *Water Traps : The Elusive Quest for Water Storage in the Chi-*
629 *Mun River Basin , Thailand. Working Paper. Mekong Program on Water, Environment and*
630 *Resilience (MPOWER). University of Natural Resources and Applied Life Sciences, Institut*
631 *de Recherche pour le. Chiang Mai, Thailand.*

- Frappart, F., Biancamaria, S., Normandin, C., Blarel, F., Bourrel, L., Aumont, M., ... Darrozes, J. (2018). Influence of recent climatic events on the surface water storage of the Tonle Sap Lake. *Science of the Total Environment*, 636, 1520–1533.
<https://doi.org/10.1016/j.scitotenv.2018.04.326>
- Frappart, F., Minh, K. Do, Hermitte, J. L., Cazenave, A., Ramillien, G., & Toan, T. Le. (2006). Water volume change in the lower Mekong from satellite altimetry and imagery data. *Geophysical Journal International*, 167, 570–584. <https://doi.org/10.1111/j.1365-246X.2006.03184.x>
- Grumbine, R. E., & Xu, J. (2011). Mekong hydropower development. *Science*, 332(6026), 178–179. <https://doi.org/10.1126/science.1200990>
- Guan, Y., & Zheng, F. (2021). Alterations in the Water-Level Regime of Tonle Sap Lake. *Journal of Hydrologic Engineering*, 26(1), 05020045.
[https://doi.org/10.1061/\(asce\)he.1943-5584.0002013](https://doi.org/10.1061/(asce)he.1943-5584.0002013)
- Halls, A. S., Paxton, B. R., Hall, N., Ngor, P. B., Lieng, S., Ngor, P., & So, N. (2013). *The stationary trawl (Dai) fishery of the Tonle Sap-Great Lake System, Cambodia*. MRC Technical Paper No. 32. Phnom Penh, Cambodia.
- Hansen, M. C., Potapov, P. V., Moore, R., Hancher, M., Turubanova, S. A., Tyukavina, A., ... Townshend, J. R. G. (2013). High-Resolution Global Maps of 21st-Century Forest Cover Change. *Science*, 850(November), 850–854. <https://doi.org/10.1126/science.1244693>
- Hecht, J. S., Lacombe, G., Arias, M. E., Dang, T. D., & Piman, T. (2019). Hydropower dams of the Mekong River basin: A review of their hydrological impacts. *Journal of Hydrology*, 568(October 2018), 285–300. <https://doi.org/10.1016/j.jhydrol.2018.10.045>
- Heinonen, U. (2006). Environmental Impact on Migration in Cambodia : Water-related Migration from the Tonle Sap Lake Region Environmental Impact on Migration in Cambodia : Water-related Migration from the Tonle Sap Lake Region. *International Journal of Water Resources Development*, 22(3), 449–462.
<https://doi.org/10.1080/07900620500482865>
- Ho, C. H., Baik, J. J., Kim, J. H., Gong, D. Y., & Sui, C. H. (2004). Interdecadal changes in summertime typhoon tracks. *Journal of Climate*, 17(9), 1767–1776.

[https://doi.org/10.1175/1520-0442\(2004\)017<1767:ICISTT>2.0.CO;2](https://doi.org/10.1175/1520-0442(2004)017<1767:ICISTT>2.0.CO;2)

- Hoang, L. P., Lauri, H., Kumm, M., Koponen, J., Vliet, M. T. H. V., Supit, I., ... Ludwig, F. (2016). Mekong River flow and hydrological extremes under climate change. *Hydrology and Earth System Sciences*, 20(7), 3027–3041. <https://doi.org/10.5194/hess-20-3027-2016>
- Hrudya, P. H., H. Varikoden, R. Vishnu. (2021). A review on the Indian summer monsoon rainfall, variability and its association with ENSO and IOD. *Meteorology and Atmospheric Physics*, 133, 1-14. <https://doi.org/10.1007/s00703-020-00734-5>
- Ji, X., Li, Y., Luo, X., & He, D. (2018). Changes in the Lake Area of Tonle Sap : Possible Linkage to Runoff Alterations in the Lancang River ? *Remote Sensing*, 10. <https://doi.org/10.3390/rs10060866>
- Junk, W., Bayley, P. B., & Sparks, R. E. (1989). The Flood Pulse Concept in River-Floodplain Systems. In *Canadian Special Publication of Fisheries and Aquatic Sciences* (Vol. 106, pp. 110–127). Retrieved from <http://www.dfo-mpo.gc.ca/Library/111846.pdf>
- Kallio, M., & Kumm, D. (2021). Comment on ‘Changes of inundation area and water turbidity of Tonle Sap Lake: responses to climate changes or upstream dam construction?’ *Environmental Research Letters* 16 058001. <https://doi.org/10.1088/1748-9326/abf3da>
- Kc, K. B., Bond, N., Fraser, E. D. G., Elliott, V., Farrell, T., McCann, K., ... Bieg, C. (2017). Exploring tropical fisheries through fishers’ perceptions: Fishing down the food web in the Tonlé Sap, Cambodia. *Fisheries Management and Ecology*, 24(6), 452–459. <https://doi.org/10.1111/fme.12246>
- Kendall, M. G. (1938). A New Measure of Rank Correlation. *Biometrika*, 30(1/2), 81. <https://doi.org/10.2307/2332226>
- Keskinen, M. (2006). The Lake with Floating Villages : Socio-economic Analysis of the Tonle Sap Lake. *International Journal of Water Resources Development*, 22(3), 463–480. <https://doi.org/10.1080/07900620500482568>
- Keskinen, M., Chinvanno, S., Kumm, M., Nuorteva, P., Snidvongs, A., Varis, O., & Västilä, K. (2010). Climate change and water resources in the Lower Mekong River Basin : putting adaptation into the context. *Journal of Water and Climate Change*, 103–118. <https://doi.org/10.2166/wcc.2010.009>

- Keskinen, M., Someth, P., Salmivaara, A., & Kummu, M. (2015). *Water-Energy-Food Nexus in a Transboundary River Basin: The Case of Tonle Sap Lake, Mekong River Basin*. *Water*. <https://doi.org/10.3390/w7105416>
- Kingston, D. G., Thompson, J. R., & Kite, G. (2011). Uncertainty in climate change projections of discharge for the Mekong River Basin. *Hydrology and Earth System Sciences*, 15(5), 1459–1471. <https://doi.org/10.5194/hess-15-1459-2011>
- Kummu, M. (2009). Water management in Angkor: Human impacts on hydrology and sediment transportation. *Journal of Environmental Management*, 90(3), 1413–1421. <https://doi.org/10.1016/j.jenvman.2008.08.007>
- Kummu, M., Keskinen, M., & Varis, O. (Eds.). (2008). *Modern Myths of the Mekong: a critical review of water and development concepts, principles and policies*. Espoo, Finland: Water & Development Publications - Helsinki University of Technology. Retrieved from [water.tkk.fi /global/publications](http://water.tkk.fi/global/publications)
- Kummu, M., & Sarkkula, J. (2008). Impact of the Mekong River flow alteration on the Tonle Sap flood pulse. *Ambio*, 37(3), 185–192. [https://doi.org/10.1579/0044-7447\(2008\)37\[185:IOTMRF\]2.0.CO;2](https://doi.org/10.1579/0044-7447(2008)37[185:IOTMRF]2.0.CO;2)
- Kummu, M., Sarkkula, J., Koponen, J., & Nikula, J. (2006). Ecosystem Management of the Tonle Sap Lake : An Integrated Modelling Approach. *International Journal of Water Resources Development*, 22(3), 497–519. <https://doi.org/10.1080/07900620500482915>
- Kummu, M., Tes, S., Yin, S., Adamson, P., Józsa, J., Koponen, J., ... Sarkkula, J. (2014). Water balance analysis for the Tonle Sap Lake – floodplain system. *Hydrological Processes*, 1733(February 2013), 1722–1733. <https://doi.org/10.1002/hyp.9718>
- Lamberts, D. (2006). The Tonle Sap Lake as a productive ecosystem. *International Journal of Water Resources Development*, 22(3), 481–495. <https://doi.org/10.1080/07900620500482592>
- Lauri, H., De Moel, H., Ward, P. J., Räsänen, T. A., Keskinen, M., & Kummu, M. (2012). Future changes in Mekong River hydrology: Impact of climate change and reservoir operation on discharge. *Hydrology and Earth System Sciences*, 16(12), 4603–4619. <https://doi.org/10.5194/hess-16-4603-2012>

- Li, J., & Zeng, Q. (2002). A unified monsoon index. *Geophysical Research Letters*, 29(8), 1–4.
<https://doi.org/10.1029/2001GL013874>
- Lin, Z., & Qi, J. (2017). Hydro-dam – A nature-based solution or an ecological problem: The fate of the Tonlé Sap Lake. *Environmental Research*, 158(October), 24–32.
<https://doi.org/10.1016/j.envres.2017.05.016>
- MRC. (2010a). *Assessment of basin-wide development scenarios technical Note 10: Impacts on the Tonle Sap Ecosystem*. Mekong River Commission. Vientiane, Lao PDR.
- MRC. (2010b). *State of the Basin Report 2010*. Mekong River Commission. Mekong River Commission. Vientiane, Lao PDR. <https://doi.org/ISSN 1728:3248>
- MRC. (2019). *State of the Basin Report 2018*. Mekong River Commission. Vientiane, Lao PDR. Retrieved from <http://www.mrcmekong.org/publications/>
- Muggeo, V. M. R. (2003). Estimating regression models with unknown break-points. *Statistics in Medicine*, 22(19), 3055–3071. <https://doi.org/10.1002/sim.1545>
- Muggeo, V. M. R. (2017). Interval estimation for the breakpoint in segmented regression: a smoothed score-based approach. *Aust. N. Z. J. Stat.*, 59, 311–322.
<https://doi.org/10.1111/anzs.12200>
- National Institute of Statistics. (2018). *Cambodia socio-economic survey 2017*. Minsitry of Planning. Phnom Penh, Cambodia. Retrieved from <https://www.nis.gov.kh/index.php/en/14-cses/12-cambodia-socio-economic-survey-reports>
- Ngor, P. B., McCann, K. S., Grenouillet, G., So, N., McMeans, B. C., Fraser, E., & Lek, S. (2018). Evidence of indiscriminate fishing effects in one of the world’s largest inland fisheries. *Scientific Reports*, 8(1), 1–12. <https://doi.org/10.1038/s41598-018-27340-1>
- Pokhrel, Y., Burbano, M., Roush, J., Kang, H., Sridhar, V., & Hyndman, D. (2018). A Review of the Integrated Effects of Changing Climate, Land Use, and Dams on Mekong River Hydrology. *Water*, 10(3), 266. <https://doi.org/10.3390/w10030266>
- Poulsen, A. F., Ouch, P., Sintavong, V., Ubolratana, S., & Nguyen, T. T. (2002). *Fish migrations of the Lower Mekong River Basin : implications for development , planning and environmental management*. MRC Technical Paper No. 8 (Vol. 17). Phnom Penh,

- Cambodia. Retrieved from <http://www.ncbi.nlm.nih.gov/pubmed/18278701>
- Räsänen, T. A., & Kummu, M. (2013). Spatiotemporal influences of ENSO on precipitation and flood pulse in the Mekong River Basin. *Journal of Hydrology*, 476, 154–168. <https://doi.org/10.1016/j.jhydrol.2012.10.028>
- Räsänen, T. A., Koponen, J., Lauri, H., & Kummu, M. (2012). Downstream Hydrological Impacts of Hydropower Development in the Upper Mekong Basin. *Water Resources Management*, 26(12), 3495–3513. <https://doi.org/10.1007/s11269-012-0087-0>
- Räsänen, T. A., Someth, P., Lauri, H., Koponen, J. Sarkkula, J., Kummu, M. (2017). Observed river discharge changes due to hydropower operations in the Upper Mekong Basin. *Journal of Hydrology*, 545, 28–41. <https://doi.org/10.1016/j.jhydrol.2016.12.023>.
- Ruiz-Barradas, A., & Nigam, S. (2018). Hydroclimate variability and change over the Mekong River basin: Modeling and predictability and policy implications. *Journal of Hydrometeorology*, 19(5), 849–869. <https://doi.org/10.1175/JHM-D-17-0195.1>
- Sakamoto, T., Van Nguyen, N., Kotera, A., Ohno, H., Ishitsuka, N., & Yokozawa, M. (2007). Detecting temporal changes in the extent of annual flooding within the Cambodia and the Vietnamese Mekong Delta from MODIS time-series imagery. *Remote Sensing of Environment*, 109(3), 295–313. <https://doi.org/10.1016/j.rse.2007.01.011>
- Salmivaara, A., Kummu, M., Varis, O., & Keskinen, M. (2016). Socio-Economic Changes in Cambodia’s Unique Tonle Sap Lake Area: A Spatial Approach. *Applied Spatial Analysis and Policy*, 9(3), 413–432. <https://doi.org/10.1007/s12061-015-9157-z>
- Sen, P. K. (1968). Estimates of the Regression Coefficient Based on Kendall’s Tau. *Journal of the American Statistical Association*, 63(324), 1379–1389. <https://doi.org/10.1080/01621459.1968.10480934>
- Senevirathne, N., Mony, K., Samarakoon, L., & Kumar Hazarika, M. (2010). Land use/land cover change detection of Tonle Sap Watershed, Cambodia. *31st Asian Conference on Remote Sensing, ACRS 2010*, 852–857. Retrieved from http://open-library.cirad.fr/e-learning/rada/res/Land_use_and_land_cover_change_of_Tonle_Sap.pdf
- Siev, S., Paringit, E. C., Yoshimura, C., & Hul, S. (2016). Seasonal changes in the inundation area and water volume of the Tonle Sap River and its floodplain. *Hydrology*, 3(4), 1–12.

<https://doi.org/10.3390/hydrology3040033>

- Song, S., Lim, P., Meas, O., & Mao, N. (2011). The agricultural land use situation on the phriphery of the Tonle Sap lake. *International Journal of Environmental and Rural Development*, 2(2), 66–71. Retrieved from <http://iserd.net/ijerd22/22066.pdf>
- Taleb, E. H., & Druyan, L. M. (2003). Relationships between rainfall and West African wave disturbances in station observations. *International Journal of Climatology*, 23(3), 305–313. <https://doi.org/10.1002/joc.883>
- Tang, Q. (2020). Global change hydrology: Terrestrial water cycle and global change. *Science China Earth Sciences*, 63(3), 459–462. <https://doi.org/10.1007/s11430-019-9559-9>
- Tangdamrongsub, N., Ditmar, P. G., Steele-Dunne, S. C., Gunter, B. C., & Sutanudjaja, E. H. (2016). Assessing total water storage and identifying flood events over Tonlé Sap basin in Cambodia using GRACE and MODIS satellite observations combined with hydrological models. *Remote Sensing of Environment*, 181, 162–173. <https://doi.org/10.1016/j.rse.2016.03.030>
- Torrence, C., & Compo, G. P. (1998). A Practical Guide to Wavelet Analysis. *Bulletin of the American Meteorological Society*, 79, 61–78. Available from <http://paos.colorado.edu/research/wavelets/>
- Uk, S., Yoshimura, C., Siev, S., Try, S., Yang, H., Oeurng, C., ... Hul, S. (2018). Tonle Sap Lake: Current status and important research directions for environmental management. *Lakes and Reservoirs: Research and Management*, 23(3), 177–189. <https://doi.org/10.1111/lre.12222>
- Vichet, N., Kawamura, K., Trong, D. P., Van On, N., Gong, Z., Lim, J., ... Bunly, C. (2019). MODIS-based investigation of flood areas in southern Cambodia from 2002–2013. *Environments - MDPI*, 6(5). <https://doi.org/10.3390/environments6050057>
- Wang, B., Wu, R., & Lau, K. M. (2001). Interannual variability of the asian summer monsoon: Contrasts between the Indian and the Western North Pacific-East Asian monsoons. *Journal of Climate*, 14(20), 4073–4090. [https://doi.org/10.1175/1520-0442\(2001\)014<4073:IVOTAS>2.0.CO;2](https://doi.org/10.1175/1520-0442(2001)014<4073:IVOTAS>2.0.CO;2)
- Wang, Y., Feng, L., Liu, J., Hou, X., & Chen, D. (2020). Changes of inundation area and water

turbidity of Tonle Sap Lake: responses to climate changes or upstream dam construction?
Environmental Research Letters, 1–30. <https://doi.org/10.1088/1748-9326/abac79>

Webster, P. J., & Yang, S. (1992). Monsoon and ENSO: Selectively interactive systems.
Quarterly Journal of the Royal Meteorological Society, 118, 877–926.
<https://doi.org/10.1256/smsqj.50704>

Wang, Y., Feng, L., Liu, J. & Chen, D. (2021). Reply to Comment on ‘Changes of inundation
 area and water turbidity of Tonle Sap Lake: responses to climate changes or upstream dam
 construction?’ *Environmental Research Letters*, 16, 058002. <https://doi.org/10.1088/1748-9326/abf3db>

Wu, F., Wang, X., Cai, Y., & Li, C. (2016). Spatiotemporal analysis of precipitation trends under
 climate change in the upper reach of Mekong River basin. *Quaternary International*, 392,
 137–146. <https://doi.org/10.1016/j.quaint.2013.05.049>

Xue, Z., Liu, J. P., & Ge, Q. (2011). Changes in hydrology and sediment delivery of the Mekong
 River in the last 50 years: Connection to damming, monsoon, and ENSO. *Earth Surface
 Processes and Landforms*, 36(3), 296–308. <https://doi.org/10.1002/esp.2036>

Yun, X., Tang, Q., Wang, J., Liu, X., Zhang, Y., Lu, H., ... Chen, D. (2020). Impacts of climate
 change and reservoir operation on streamflow and flood characteristics in the Lancang-
 Mekong River Basin. *Journal of Hydrology*, 590, 125472.
<https://doi.org/10.1016/j.jhydrol.2020.125472>

Yun, X., Tang, Q., Li, J., Lu, H., Zhang, L., & Chen, D. (2021). Can reservoir regulation
 mitigate future climate change induced hydrological extremes in the Lancang-Mekong
 River Basin?. *Science of The Total Environment*, 785, 147322.
<https://doi.org/10.1016/j.scitotenv.2021.147322>

Zeng, Z., Estes, L., Ziegler, A. D., Chen, A., Searchinger, T., Hua, F., ... F. Wood, E. (2018).
 Highland cropland expansion and forest loss in Southeast Asia in the twenty-first century.
Nature Geoscience, 11(8), 556–562. <https://doi.org/10.1038/s41561-018-0166-9>

Ziv, G., Baran, E., Nam, S., Rodriguez-Iturbe, I., & Levin, S. A. (2012). Trading-off fish
 biodiversity, food security, and hydropower in the Mekong River Basin. *Proceedings of the
 National Academy of Sciences*, 109(15), 5609–5614.

834 <https://doi.org/10.1073/pnas.1201423109>

Supporting Information

Multidecadal variability of the Tonle Sap Lake flood pulse regime

Aifang Chen^{1,2}, Junguo Liu^{1*}, Matti Kummu³, Olli Varis³, Qiuhong Tang^{4,5}, Ganquan Mao¹, Jie Wang⁴, Deliang Chen^{2*}

¹School of Environmental Science and Engineering, Southern University of Science and Technology, Shenzhen 518055, China

²Regional Climate Group, Department of Earth Sciences, University of Gothenburg, Gothenburg 40530, Sweden

³Water and Development Research Group, Aalto University, P.O. Box 15200, Aalto, Finland

⁴Key Laboratory of Water Cycle and Related Land Surface Processes, Institute of Geographic Sciences and Natural Resources Research, Chinese Academy of Sciences, Beijing 100101, China

⁵University of Chinese Academy of Sciences, Beijing 100101, China

*Corresponding author: Junguo Liu (junguo.liu@gmail.com), Deliang Chen (deliang@gvc.gu.se)

Present address: School of Environmental Science and Engineering, Southern University of Science and Technology, Shenzhen 518055, China

Contents of this file

Figures S1 to S5

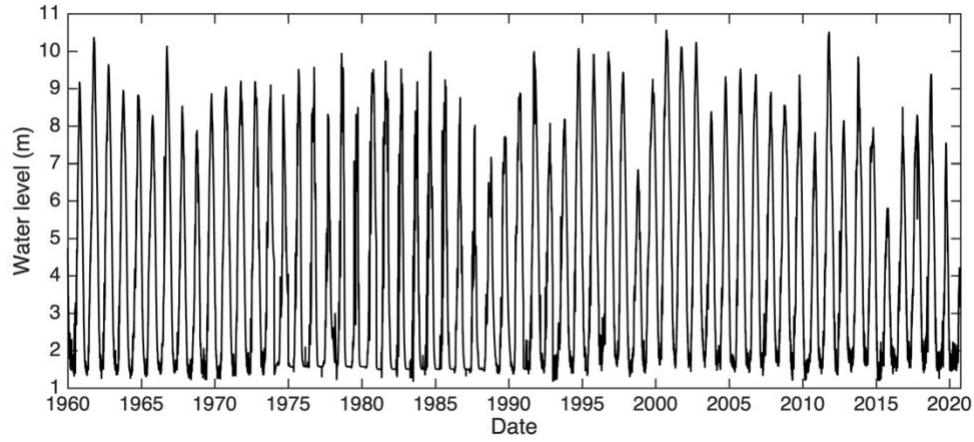


Figure S1. Time series of estimated daily water level at Kompong Luong station based on multiple polynomial regression for 1960 – 2020.

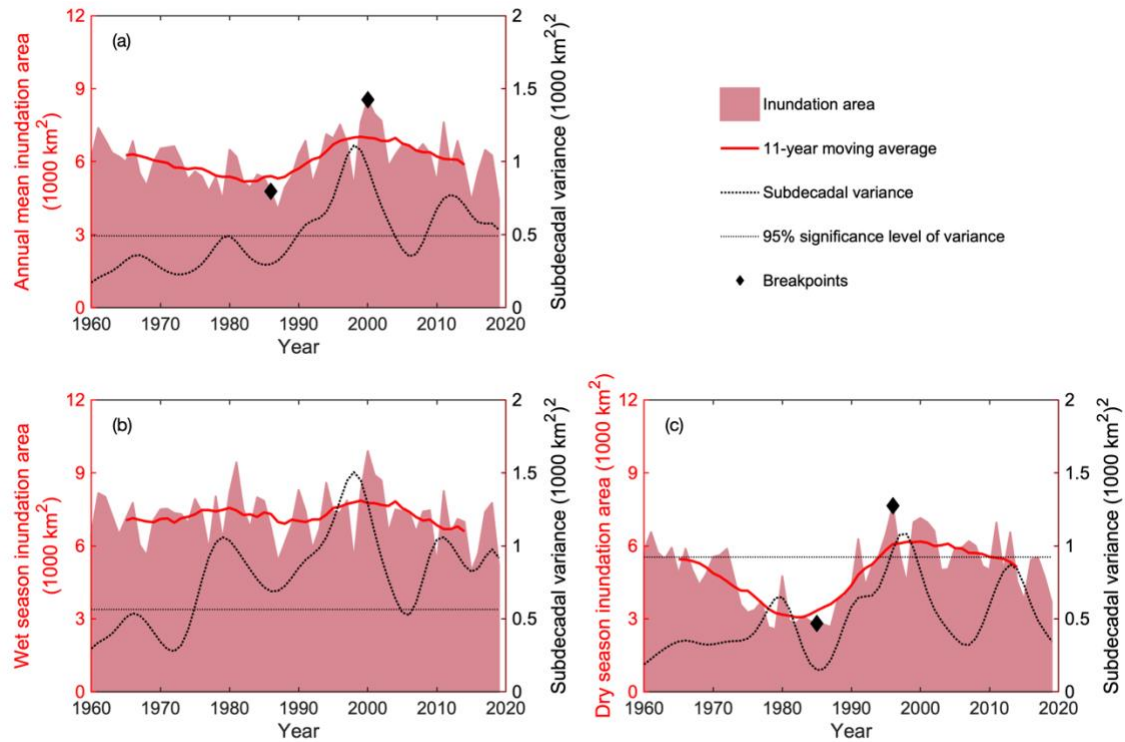


Figure S2. Time series of inundation area of the Tonle Sap Lake for 1960 – 2019. Mean inundation area in (a) annual, (b) wet season (May – October), and (c) dry season (November – April). The red line is the 11-year moving average of inundation area time series, whereas the black line represents the subdecadal variance (variance of scales lower than 10 years) of the inundation area estimated by wavelet analysis, with significance area of 95% shown in black dash line. The breakpoints are marked with diamond markers determined with R package ‘segmented’ (Muggeo, 2003, 2017).

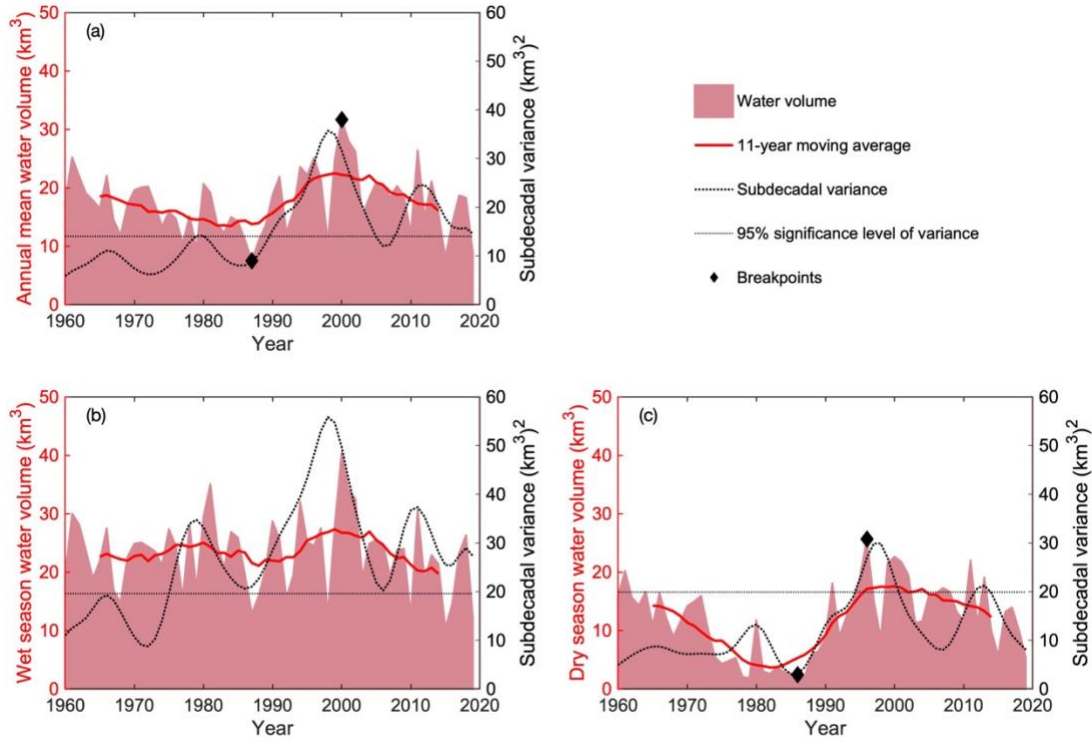


Figure S3. Time series of water volume of the Tonle Sap Lake for 1960 – 2019. Mean water volume in (a) annual, (b) wet season (May – October), and (c) dry season (November – April). The red line is the 11-year moving average of water volume time series, whereas the black line represents the subdecadal variance (variance of scales lower than 10 years) of the water volume estimated by wavelet analysis, with significance area of 95% shown in black dash line. The breakpoints are marked with diamond markers determined with R package ‘segmented’ (Muggeo, 2003, 2017).

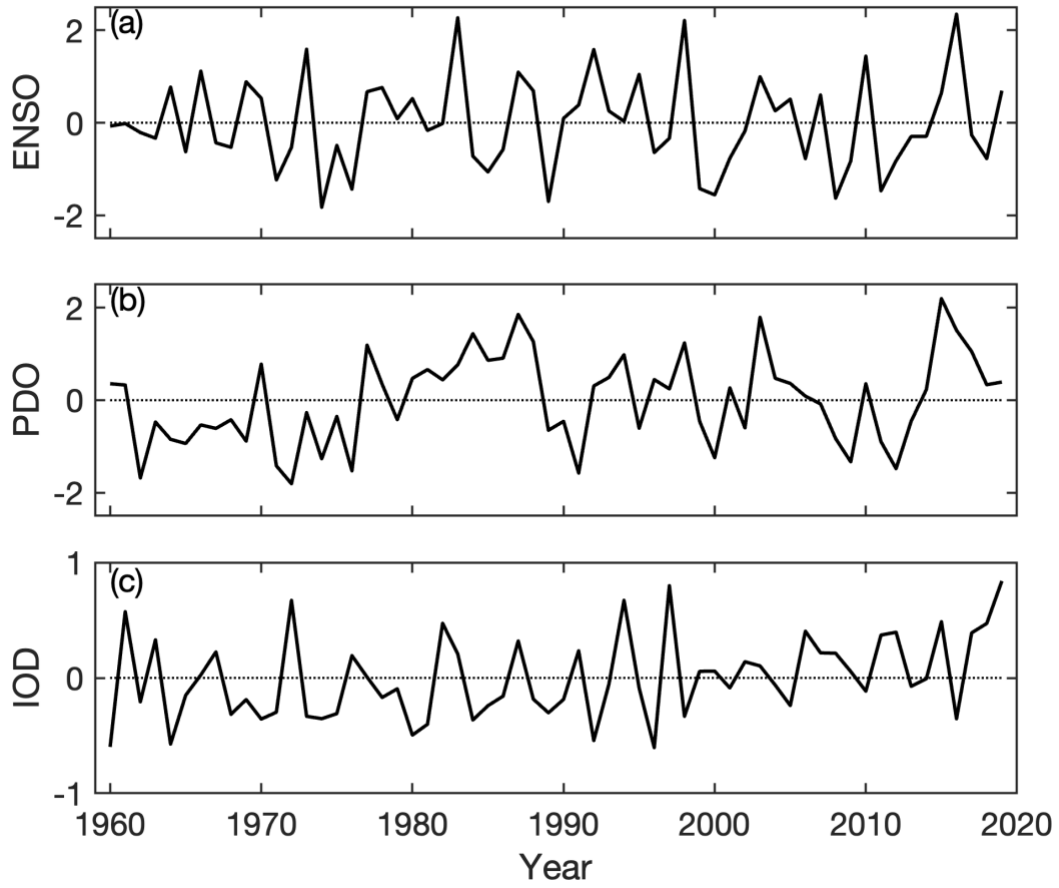


Figure S4. Time series of the atmospheric circulations: El Niño-Southern Oscillation (ENSO, a), Pacific Decadal Oscillation (PDO, b), and Indian Ocean Dipole (IOD, c) for 1960 – 2019.

The wavelet coherence method is often used to estimate covariance between two time series, which are co-varying (Grinsted, Moore, & Jevrejeva, 2004; Jevrejeva, Moore, & Grinsted, 2003; Torrence & Compo, 1998). To understand the influence of atmospheric circulations on the flood pulse of the TSL, we employed the wavelet coherence to identify the covariances of WL_wet and each of the three circulation indices (ENSO, PDO, and IOD) at frequency and time intervals, respectively. We found that WL_wet and atmospheric circulations have significant coherencies at a frequency of two- to fourteen-years periods, indicating co-varying water level of the TSL and atmospheric circulations.

The vectors represented the phase difference between WL_wet and each of the atmospheric circulations. We found that both ENSO and PDO were anti-phase with WL_wet when significantly coherent, indicating that wet years with high water levels tend to be associated with cold events and vice versa. IOD and WL_wet were anti-phase before the mid-1980s. However, it changed to in-phase during the late 1990s. This means that wet years used to be associated with the negative phase of IOD (warm water in the eastern Indian Ocean), but it became associated with the positive phase of IOD (cold water in the eastern Indian Ocean). Overall, the results indicate that the atmospheric circulations have influenced the water level of the TSL in different time scales.

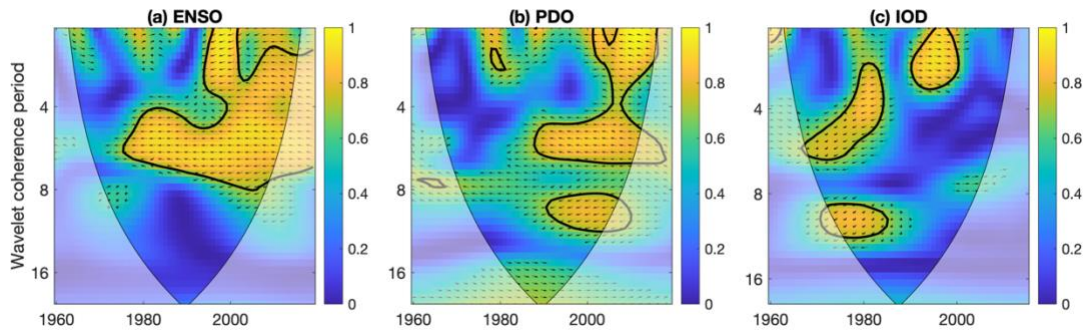


Figure S5. Wavelet coherence spectrum between the wet season water level of the Tonle Sap Lake and each of the large-scale atmospheric circulations, including El Niño-Southern Oscillation (ENSO, a), Pacific Decadal Oscillation (PDO, b), and Indian Ocean Dipole (IOD, c) for 1960 – 2019. Thick black contours enclose times and frequencies with significant phase coherence at 5% significance level. The relative phase relationship between two periodic signals is represented by the arrows (with the arrow to the right [left] indicating in-phase [anti-phase]).

References

- Grinsted, A., Moore, J. C., & Jevrejeva, S. (2004) Application of the cross wavelet transform and wavelet coherence to geophysical time series. *Nonlinear Processes in Geophysics*, 11, 561–566. <https://doi.org/10.5194/npg-11-561-2004>.
- Jevrejeva, S., Moore, J. C., & Grinsted, A. (2003) Influence of the Arctic Oscillation and El Niño-Southern Oscillation (ENSO) on ice conditions in the Baltic Sea: The wavelet approach. *Journal of Geophysical Research: Atmospheres*, 108, 1–11. doi:10.1029/2003JD003417, D21.
- Muggeo, V. M. R. (2003). Estimating regression models with unknown break-points. *Statistics in Medicine*, 22(19), 3055–3071. <https://doi.org/10.1002/sim.1545>
- Muggeo, V. M. R. (2017). Interval estimation for the breakpoint in segmented regression: a smoothed score-based approach. *Aust. N. Z. J. Stat.*, 59, 311–322. <https://doi.org/10.1111/anzs.12200>
- Torrence, C., & Compo, G. P. (1998). A Practical Guide to Wavelet Analysis. *Bulletin of the American Meteorological Society*, 79, 61–78. Available from <http://paos.colorado.edu/research/wavelets/>